Journal of Building Engineering 43 (2021) 102591

Contents lists available at ScienceDirect

Journal of Building Engineering

journal homepage: www.elsevier.com/locate/jobe

Decoupling the heat loss coefficient of an in-use office building into its transmission and infiltration heat loss coefficients

Irati Uriarte *, Aitor Erkoreka, Asier Legorburu, Koldo Martin-Escudero, Catalina Giraldo-Soto, Moises Odriozola-Maritorena

ENEDI Research Group, Energy Engineering Department, University of the Basque Country (UPV/EHU), Plaza Ingeniero Torres Quevedo 1, 48013, Bilbao, Spain

ARTICLE INFO

Keywords:
Energy performance gap
Heat loss coefficient (HLC)
Transmission (UA value) and infiltration (C_v) heat loss coefficient
Metabolic CO_2 decay
Decoupling HLC

ABSTRACT

The actual building energy performance essentially depends on the building occupant's behaviour, the real performance of the installed energy systems and the in-use performance of the building envelope. The thermal performance characterization of in-use building envelopes, based on monitored data, represents a crucial step towards bridging the gap between the designed and as-built energy performance of buildings. The main indicator to analyse the performance gap of building envelopes is the Heat Loss Coefficient (HLC); when measured, it commonly shows considerable differences when compared with the design value. This research goes further and proposes a method, based on monitored data from in-use buildings, for the decoupling of the HLC of in-use buildings into its transmission (UA) and infiltration (C_v) heat loss coefficients, in order to identify the origin of the heat losses. The identification of this origin will facilitate the reduction of the performance gap. Therefore, a multi-storey occupied office building of the University of the Basque Country has been monitored and analysed, where the in-use HLC for each floor and for the whole building have already been estimated using an average method. Then, based on the ASTM D6245-18 Standard, the decay method of the metabolic CO_2 of the building's occupants has been successfully applied in this paper to obtain the Air Change per Hour (ACH) rates due to infiltrations. These ACH values have been used to decouple the estimated HLC values into their transmission and infiltration parts.

1. Introduction

The high building energy consumption and its corresponding CO_2 emissions has driven the European Union to implement several regulations concerning energy efficiency in buildings [1]. These regulations are commonly based on design period estimations. Unfortunately, the design energy consumption values and the real energy consumption values often show a considerable difference [2–4], the so-called energy performance gap. A considerable part of this energy performance gap is due to the difference between the building's real envelope energy performance as compared to the expected performance of the design phase. The most common performance indicator used to describe a building's envelope energy performance is the Heat Loss Coefficient (HLC).

This coefficient is the sum of two heat loss coefficients representing two phenomena occurring through the envelope of the building [5]. The first coefficient is the transmission heat loss coefficient (UA), which considers the heat transmission occurring through the envelope of the building. The transmission heat loss coefficient is mainly dependent on the thermal conductivity and thickness of the building envelope materials. It can be measured in-situ for such components as windows, walls, roofs … [6,7], as the U-value can be estimated by measuring the inner surface heat flux and the outdoor and indoor temperatures. However, the proper and accurate in-situ measurement of the UA value for a complete building envelope can be time consuming and quite expensive if the aforementioned method is used [8].

On the other hand, the second coefficient that makes up the total heat loss coefficient is the infiltration and/or ventilation heat loss coefficient (C_v), which depends on the airtightness and ventilation system performance of the corresponding building. Infiltrations can be defined as the uncontrolled air movements across the building through unintentional openings or cracks, while ventilation is an intentional renovation of the indoor air through outdoor airflows entering the building in order to improve the indoor air quality. The ventilation can be natural (through window opening) and driven by the weather conditions or mechanical ventilation (through a ventilation system) [9–11].

* Corresponding author.
E-mail address: irati.uriarte@ehu.eus (I. Uriarte).

https://doi.org/10.1016/j.jobe.2021.102591
Received 17 February 2021; Received in revised form 15 April 2021; Accepted 17 April 2021
Available online 30 April 2021

Abbreviations and units

ACH Air Changes per Hour, or air change renovation rate of the considered volume [h^{-1}]

$ACH_{building}$ The Air Change per Hour of the whole building [h^{-1} or s^{-1}]

ACH_{decay} The Air Change per Hour estimated using the CO_2 tracer gas decay method of the considered volume [h^{-1}]

$ACH_{Fi,j}$ The corresponding Air Change per Hour of the i^{th} zone of the j^{th} floor [h^{-1} or s^{-1}]

ACH_{Fi,j_decay} The corresponding Air Change per Hour estimated using the CO_2 tracer gas decay method of the i^{th} zone of the j^{th} floor [h^{-1} or s^{-1}]

ACH_{decay_aver} The entire floor average Air Change per Hour estimated using the CO_2 tracer gas decay method for the whole considered testing period in [h^{-1}]

$ACH_{decay\_aver\_Vi}$ The average Air Change per Hour estimated using the CO_2 tracer gas decay method of the whole considered testing period associated with each 'i' volume portion of F0 and F2, respectively, in [h^{-1}]

ACH_{decay_Vi} The daily Air Change per Hour estimated using the CO_2 tracer gas decay method of the whole considered testing period associated with each of the 'i' volume portions of F0 and F2, respectively, in [h^{-1}]

C_F Final indoor to outdoor concentration difference [ppm, $\frac{mol_{CO2}}{mol_{air}}, \frac{m^3_{CO2}}{m^3_{air}}$]

$C_{Fbuilding}$ Final indoor to outdoor concentration difference for the whole building [ppm, $\frac{mol_{CO2}}{mol_{air}}, \frac{m^3_{CO2}}{m^3_{air}}$]

$C_{FFi,j}$ Final indoor to outdoor concentration difference of the i^{th} zone of the j^{th} floor [ppm, $\frac{mol_{CO2}}{mol_{air}}, \frac{m^3_{CO2}}{m^3_{air}}$]

C_I Initial indoor to outdoor concentration difference [ppm, $\frac{mol_{CO2}}{mol_{air}}, \frac{m^3_{CO2}}{m^3_{air}}$]

$C_{Ibuilding}$ Initial indoor to outdoor concentration difference for the whole building [ppm, $\frac{mol_{CO2}}{mol_{air}}, \frac{m^3_{CO2}}{m^3_{air}}$]

$C_{IFi,j}$ Initial indoor to outdoor concentration difference of the i^{th} zone of the j^{th} floor [ppm, $\frac{mol_{CO2}}{mol_{air}}, \frac{m^3_{CO2}}{m^3_{air}}$]

CO_2 Carbon dioxide.

Cp_{air} Constant pressure specific heat of the air at the average indoor temperature [kJ/kgK]

C_v Infiltration ($C_{v\text{-}inf}$) and/or ventilation ($C_{v\text{-}vent}$) heat loss coefficient [kW/K]

C_{v_aver} The entire floor average infiltration heat loss coefficient for the whole considered testing period [kW/K]

$C_{v\ Fi,j\text{-}out}$ Considers the envelope infiltration and/or ventilation heat loss coefficient going from the i^{th} zone of the j^{th} floor to the exterior [kW/K]

Δt Time frequency at which each discrete measurement is done [h]

η Efficiency of the recovery system installed in the ventilation system [−]

Fi,j The i^{th} zone of the j^{th} floor in a building

Fn Corresponding floor of the analysed building (F0 (ground floor), F1 (first floor), F2 (second floor) and F3 (third floor))

HLC (Heat Loss Coefficient) Considers transmission heat losses through the building envelope plus infiltration and/or ventilation heat losses per degree of difference between indoor and outdoor temperatures. HLC = UA + C_v [kW/K]

$HLC_{Fi,j}$ Heat Loss Coefficient of the i^{th} zone of the j^{th} floor [kW/K]

HLC_{sum} Heat Loss Coefficient calculated as the sum of each individual thermal zone HLC [kW/K]

K All the other heat gains inside the building excluding solar gains (S_aV_{sol}) and all heating system gains (Q) [kW]. K = $K_{electricity}$ + $K_{occupancy}$

$K_{electricity}$ Heat gains inside the building due to electricity consumed within the building envelope [kW]

$K_{Fi,j}$ All the other heat gains inside the i^{th} zone of the j^{th} floor excluding solar gains (S_aV_{sol}) and all heating system gains (Q) [kW]

$K_{occupancy}$ Heat gains inside the building due to metabolic generation of the occupants [kW]

$\dot{m}$ Air mass flow rate [kg/s]

$\dot{m}_{Fi,j-Fi,j}$ Mass flow rate of the air going from the i^{th} zone of the j^{th} floor to other i^{th} zone of the same or a different j^{th} floor [kg/s]

$\dot{m}_{Fi,j-out}$ Mass flow rate of the air going from the i^{th} zone of the j^{th} floor to the exterior. In the case the air goes from the exterior to the i^{th} zone of the j^{th} floor, it will be named as $\dot{m}_{out-Fi,j}$ [kg/s]

n_{air} The total number of moles of air within the whole building [mol]

$n_{CO2,F,building}$ The total number of moles of CO_2 within the whole building at the end of the decay analysis period (t = t [s]) [mol]

$n_{CO2,I,building}$ The total number of moles of CO_2 within the whole building at the beginning of the decay analysis period (t = 0 [s]) [mol]

P_{in} Pressure inside the building [bar]

P_{out} Pressure outside the building [bar]

Q *or* $Q_{heating}$ All heating systems' energy inputs inside the building [kW]

$Q_{Fi,j}$ All heating systems' energy inputs inside the i^{th} zone of the j^{th} floor [kW]

$Q_{infiltration}$ Heat losses of the building due to infiltrations [kW]

$Q_{inf\ +\ vent}$ Sum of $Q_{infiltration}$ and $Q_{ventilation}$ [kW]

$Q_{transmission}$ Heat losses of the building due to transmission [kW]

$Q_{ventilation}$ Heat losses of the building due to ventilation systems [kW]

ρ_{air} Density of the air at the building average indoor temperature and pressure [kg/m^3]

ρ_{CO2} Density of the CO_2 at the building average indoor temperature and pressure [kg/m^3]

S_aV_{sol} Corresponding solar gains of the building [kW]

$(S_aV_{sol})_{Fi,j}$ Corresponding solar gains of the i^{th} zone of the j^{th} floor [kW]

SF_6 Sulphur hexafluoride.

t Duration of the CO_2 concentration decay analysis [h]

T_{exh} Temperature of the exhausted air after crossing the heat recovery system [K or °C]

$T_{Fi,j}$ Indoor temperature of the i^{th} zone of the j^{th} floor [K or °C]

T_{ground} Ground temperature [K or °C]

T_{in} Indoor air temperature [K or °C]

T_{out} Outdoor air temperature [K or °C]

T_{sup} Temperature of the supply air after crossing the heat recovery system [K or °C]

U-value Building envelope element transmittance [W/m^2K]

UA Considered building envelope transmission heat loss coefficient [kW/K]

$UA_{Fi,j\text{-}ground}$ Considers the envelope transmission heat loss coefficient going from the i^{th} zone of the j^{th} floor to the ground [kW/K]

$UA_{Fi,j\text{-}Fi,j}$ Considers the envelope transmission heat loss coefficient going from the i^{th} zone of the j^{th} floor to other i^{th} zone of the same or a different j^{th} floor [kW/K]

$UA_{Fi,j\text{-}out}$ Considers the envelope transmission heat loss coefficient going from the i^{th} zone of the j^{th} floor to the exterior [kW/K]

$\dot{V}$ Volumetric airflow rate [m^3/h]

$\dot{V}_{air(inf)}$	Infiltration volumetric air flow rate [m^3/h]
$\dot{V}_{air(vent)}$	Ventilation volumetric air flow rate [m^3/h]
$\dot{V}_{building}$	Total volumetric air flow rate of the whole building [m^3/h or m^3/s]
$\dot{V}_{Fi,j}$	The volumetric air flow rate of the i^{th} zone of the j^{th} floor [m^3/h or m^3/s]
$\dot{V}_{Fi,j\_decay}$	The volumetric air flow rate estimated using the CO_2 tracer gas decay method of the i^{th} zone of the j^{th} floor [m^3/h or m^3/s]
$\dot{V}_{Fi,j-Fi,j}$	Volumetric air flow rate going from the i^{th} zone of the j^{th} floor to other i^{th} zone of the same or a different j^{th} floor [m^3/h or m^3/s]
$\dot{V}_{Fi,j-out}$	Volumetric air flow rate going from the i^{th} zone of the j^{th} floor to the exterior. In the case the air goes from the exterior to the i^{th} zone of the j^{th} floor, it will be named as $\dot{V}_{out-Fi,j}$ [m^3/h or m^3/s]
$V_{ol\_building}$	The total volume of the building [m^3]
$V_{ol\_Fi,j}$	The volume of the i^{th} zone of the j^{th} floor [m^3]
V_{ol_floor}	The volume of each floor [m^3]
V_{ol_i}	The volume portion of each floor [m^3]
V_{sol}	Vertical south global solar radiation [W/m^2]
WB	West block
WS	Wind speed [m/s]

Therefore, infiltrations are a consequence of the air pressure difference between the interior and exterior, dependent on such climatic conditions as wind speed and temperature difference between the interior and exterior [12]; while the behaviour of the occupants, such as window and door opening and/or the performance of the ventilation system, will be directly related to the ventilation part [13,14]. The estimation of this heat loss coefficient can be carried out by multiplying the volumetric airflow rate ($\dot{V}$) by the air ρ_{air} and Cp_{air} (the density and constant pressure specific heat of the air at the average indoor temperature) [5]. This volumetric airflow rate is the multiplication of the Air Change per Hour (ACH) and the volume of the analysed room or building. Note that, when ventilation systems with heat recovery are present, the heat recovery efficiency must be considered when calculating the ventilation part of the infiltration and/or ventilation heat loss coefficient.

The ACH is commonly studied by the researchers working in the Indoor Air Quality field. The ACH [10] represents the total rate of outdoor air entering the building, normally considering both the ventilation and the infiltration air rates. There are two main techniques to estimate the ACH values of a building. Tracer gas techniques are based on the mass conservation of a tracer gas, which is injected into the studied zone or building and uniformly mixed. The injection method defines the tracer gas techniques, which are concentration decay [15–17], constant injection and constant concentration techniques [18]. Despite some analysis tent to compare the methods with each other [19–21], the most commonly used method individually is the concentration decay method, since it needs less tracer gas and is the easiest to perform. Moreover, the gases used for this analysis are usually inert. The most commonly used gases are sulphur hexafluoride (SF_6) [18,20,21] or carbon dioxide (CO_2) [19,22,23]. However, CO_2 is the cheapest and most easily measurable tracer gas for in-use buildings, since it is also generated by the occupants [15,24].

The ACH measured using tracer gas techniques is the actual value in an enclosure for a given set of conditions during the test: air infiltration characteristics, climatic influences, ventilation system operation, etc. Therefore, when those conditions change, the ACH value will also change. To overcome this drawback, one approach is to measure ACH under different boundary conditions trying to cover a wide range of conditions; another approach is to build a ventilation model.

The blower door test [9,25,26] does not measure the ACH in actual boundary conditions of the enclosure, the ACH is measured for several indoor/outdoor pressure differences of the building. The aim is to characterise the air permeability of the enclosure envelope, and thus, to measure the airtightness of the building envelope, as done in Ref. [27] to improve it after the rehabilitation. By the data obtained from the test and defining the behaviour of the ventilation system, it is possible to build a ventilation model and, once validated, to analyse the ACH under different sets of conditions.

Although the ACH and the HLC [28–32] are two parameters which have been widely analysed separately, as far as the authors know, they have not yet been related to decouple the HLC into its transmission (UA) and infiltration and/or ventilation (C_v) parts using in-situ measurements on in-use buildings by means of basic monitoring systems. This paper is focussed on developing a new decoupling method that could be implemented in real world scenarios through the use of simple sensors for monitoring in-use buildings. Metabolic CO_2 will be used as a tracer gas to estimate air infiltration and/or ventilation rates by means of CO_2 decay analysis. The CO_2 concentration can be easily and accurately measured by simple air quality sensors. This work is based on the requirements described in the ASTM D6245-18 'Standard Guide for Using Indoor Carbon Dioxide Concentrations to Evaluate Indoor Air Quality and Ventilation' [33]. Although the objective of this Standard is not to decouple the HLC, one of its by-products is the estimation of the Air Change per Hour (ACH) of the analysed volume (usually a thermal zone of a building). This ACH value can be used to estimate the infiltration and/or ventilation heat loss coefficient (C_v) of the studied volume. Since HLC = UA + C_v, if HLC and C_v are estimated, then the HLC may be decoupled into its transmission (UA) and infiltration and/or ventilation (C_v) parts.

The application of the proposed decoupling method requires the estimation of the HLCs of the different thermal zones or volumes to be analysed, where corresponding C_v values will also be estimated. In this work, the volumes will be the four floors of the building already studied in Refs. [5,30]. The HLC values estimated by applying the average method in Ref. [5] will be used to decouple those already estimated HLC values into the C_v and UA values.

Thus, the main objective of this paper is to apply and test the proposed CO_2 concentration decay method to decouple the in-use HLC into its UA and C_v values of an in-use office building by means of monitored data. The decoupling of the HLC would allow a clear identification of the main origin of the heat losses. In other words, it would be possible to estimate which of the heat losses are higher; the transmission heat losses or the infiltration and/or ventilation heat losses.

Moreover, it must be said that the HLC values of the building have already been estimated for two different periods in Ref. [5], one before and the other after the building was rehabilitated. Before rehabilitation, there was no ventilation system installed in the building. So, the C_v values obtained during the pre-retrofitting winters will only consider the infiltration heat losses of the building. However, after the rehabilitation, a ventilation system was installed on each of the floors. Thus, the obtained C_v during the post-retrofitting winter periods should consider both the infiltration and ventilation heat losses. However, due to the high quantity of information and data, this paper will only perform the decoupling for the HLC values obtained before the rehabilitation, proposing the decoupling of the post-rehabilitation HLC values as future work.

2. Building description and experimental set-up

2.1. Description of the building

The energy characterization presented in this document has been carried out in an energetically monitored public building of the University of the Basque Country (see Fig. 1). For this study, only the West Block (WB) has been considered. Since the West Block (WB) thermal zones are separated by "always closed" fire doors, the air mass exchanges with the central block can be considered negligible. Furthermore, both blocks have similar indoor temperature settings, so the energy exchange between blocks can also be considered insignificant. Thus, the West Block has been treated as if it was completely isolated from the central block. This West Block has four floors. Two, the first and third floors (F1 and F3), are mainly large, open offices, while the other two, the ground and second floors (F0 and F2), are mainly smaller, individual offices. The structure of the floors is important when it comes to the infiltration and/or ventilation heat loss coefficients estimation.

2.2. Description of the monitoring system

Before the rehabilitation, the building had an energy monitoring system that included several sensors located inside and outside the building. The summary of all the sensors installed in the building can be found in Table 1 of [5], showing three main types of sensor; those that measure energy consumption, indoor conditions and external (or weather) conditions. Depending on the configuration of each floor, a different number of comfort parameter measurement points have been distributed in different locations inside the building (three or four per floor, see Fig. 2). Within these comfort parameters, only the air quality (CO_2 concentration) measuring sensor is indispensable for the estimation of the C_v. However, the rest of the data measured inside the building were indispensable when estimating the HLC values presented in Ref. [5].

Data from weather measurements sensors located on the roof of the building were also available. Although a wide range of data was measured on the roof for the estimation of the HLC, the only variables needed for this study are the external temperature and wind speed. All the data have been measured minutely.

The total volumes of the monitored thermal zones (see green contour line of Fig. 2) are shown in Table 1. Table 2 only describes the number, type and characteristics of the different sensors used for C_v calculation purposes in this research work.

According to the ASTM D6245-18 guide and the Test Method ASTM E741-11 [34], in order to estimate the Air Change per Hour of a certain thermal zone, it is necessary to measure the CO_2 concentration in at least three points of the analysed thermal zones or floors. In this work three or four measurements points have been installed per analysed thermal zones (see Fig. 2). Note that the infiltration rates of a building can be altered depending on the indoor to outdoor temperature difference and with the wind speed effect. Although these data are not used in the C_v calculation, they are still needed to filter the data or check the correlation between the estimated ACH values and wind speed.

3. Heat loss coefficient (HLC) decoupling methodology

3.1. HLC estimation method of in-use buildings with multiple thermal zones

The strict metabolic CO_2 concentration homogeneity requirements presented in section 3.2 to obtain the infiltration/ventilation heat loss coefficient, makes it nearly impossible to obtain them in a whole building basis. Thus, it is needed to obtain them in a thermal zone basis. Of course, there might be heat and mass transfer between thermal zones within a building, this is why, in this subsection, the HLC estimation method is briefly presented and the key aspects regarding the heat and mass exchanges between thermal zones within a building are related to the HLC estimation and decoupling.

First of all, the method for HLC estimation of an in-use building with a unique thermal zone with homogeneous indoor temperature is presented. Let us review the principal energy and mass exchanges occurring through this in-use building envelope in heating season, see Fig. 3 (LEFT). There are different energy gains within the building: heating and ventilation system heat input provided typically by water or glycol-water as heat transfer fluid ($Q_{heating}$), metabolic heat gain produced by building users ($K_{occupancy}$), electricity heat gains produced by all the electrical devices consuming and dissipating electricity within the building envelope ($K_{electricity}$) and possible solar gains (S_aV_{sol}). We also have heat losses through the envelope due to:

- *Transmission effects* ($Q_{transmission}$) dependant on the building envelope UA value and the T_{in} to T_{out} temperature difference (equation in bold of Fig. 3).
- *Infiltration effects* ($Q_{infiltration}$) dependant on the infiltration heat loss coefficient ($C_{v\text{-}inf}$) which depends on the building envelope total permeability to the air infiltration that will produce different infiltration volumetric air flow rates $\dot{V}_{air(inf)}$ (also dependant on wind speed, direction, and T_{in} to T_{out} temperature difference) and proportional to the air density (ρ_{air}), to the air constant pressure specific heat (cp_{air}) and the T_{in} to T_{out} temperature difference (see equation in Fig. 3).
- *Ventilation effects* ($Q_{ventilation}$) dependant on the ventilation heat loss coefficient ($C_{v\text{-}vent}$) which depends on the ventilation volumetric air flow rates $\dot{V}_{air(vent)}$ (ventilation rates could be constant and scheduled or controlled by some indoor parameter such as indoor CO_2 concentration or relative humidity) and proportional to the (if

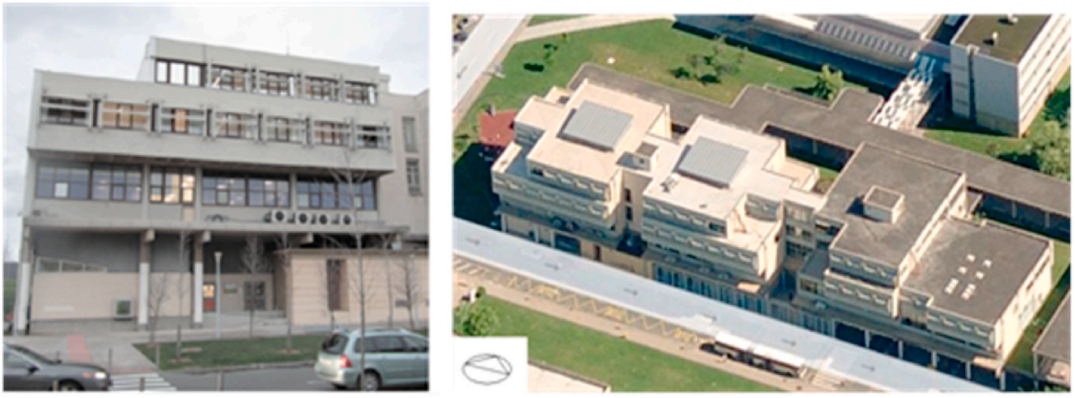

Fig. 1. South façade of the WB (left). Roof, East façade and South façade (long one) of the whole building (right).

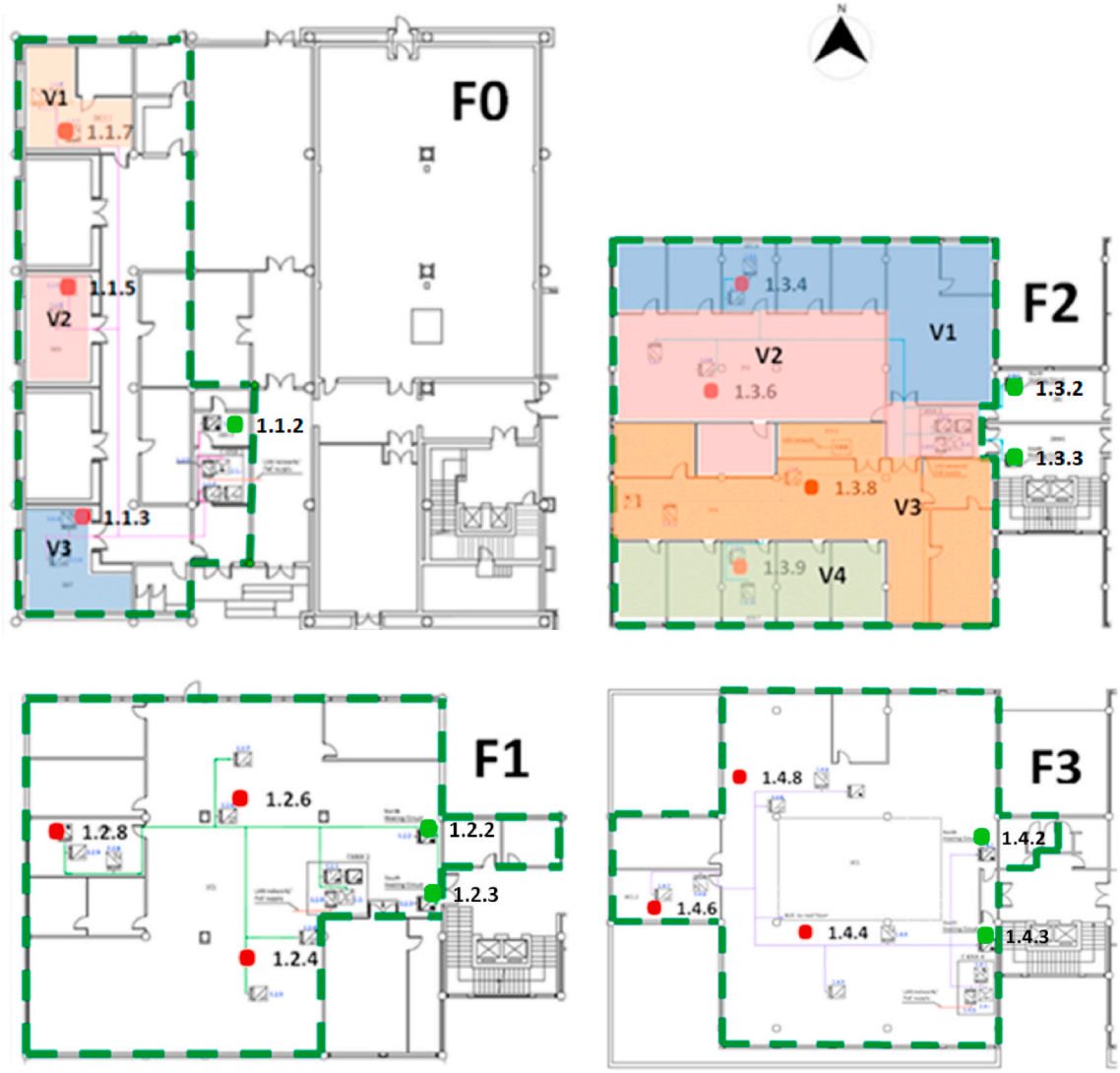

Fig. 2. Distribution of monitoring devices within the considered thermal zones of the building. RED DOT: locations where brightness level, air quality (CO_2 ppm), temperature and relative humidity have been measured. GREEN DOT: calorimeter positions. Representation of volume partitions considered in F0 and F2 for C_v calculation purposes are also highlighted. (For interpretation of the references to colour in this figure legend, the reader is referred to the Web version of this article.)

Table 1
Monitored total volumes for each thermal zone (floors in this case) and for the building.

	V_{ol_floor} [m^3]
FLOOR 0	1184.3
FLOOR 1	1700.2
FLOOR 2	1889.7
FLOOR 3	1619.3
BUILDING	**6393.5**

existing) heat recovery efficiency (η), to ρ_{air}, to cp_{air} and to the T_{in} to T_{out} temperature difference (see equation in Fig. 3).

If we sum, as in Fig. 3 bold equation, $Q_{inf\ +\ vent} = Q_{infiltration} + Q_{ventilation}$, taking ($T_{in} - T_{out}$) as common factor, and reordering, we get Eq. (1) for the most general case for the whole building infiltration/ventilation heat loss coefficient. Note that buildings without heat recovery in their ventilation system are represented by $\eta = 0$. Of course, in buildings without ventilation system, only the infiltration term remains.

$$C_v = \dot{V}_{air(vent)}\rho_{air}cp_{air}\cdot(1-\eta) + \dot{V}_{air(inf)}\rho_{air}cp_{air}\ [kW/K] \qquad \text{Eq. (1)}$$

Table 2
Summary of the sensor information used to generate the input data required to carry out this research.

MEASUREMENT		DEVICE IDENTIFICATION	ACCURACY
Indoor Conditions	**Air Quality (ppm CO_2)**	13 Air quality, Temperature and Humidity Sensors: **ARCUS SK04–S8–CO2-TF**	**± 1 % Measurement Error**
	Temperature (°C)		±0.5 °C
	Relative Humidity (%)		±3 % RH
Outdoors Conditions	Temperature (°C)	1 Weather Station on roof: **ELSNER 3595 Suntracer KNX basic**	±0.5 °C
	Wind Speed (m/s)		**±25 % at 0 … 15 m/s**
	Temperature (°C)	1 Outdoor Temperature and Humidity Sensor on roof: **ARCUS SK01-TFK-AFF**	**± 0.5 °C**

The so called average method to estimate the HLC of the building, applies the energy conservation principle to the building schematic of Fig. 3. This energy conservation equation analysis (developed in detail

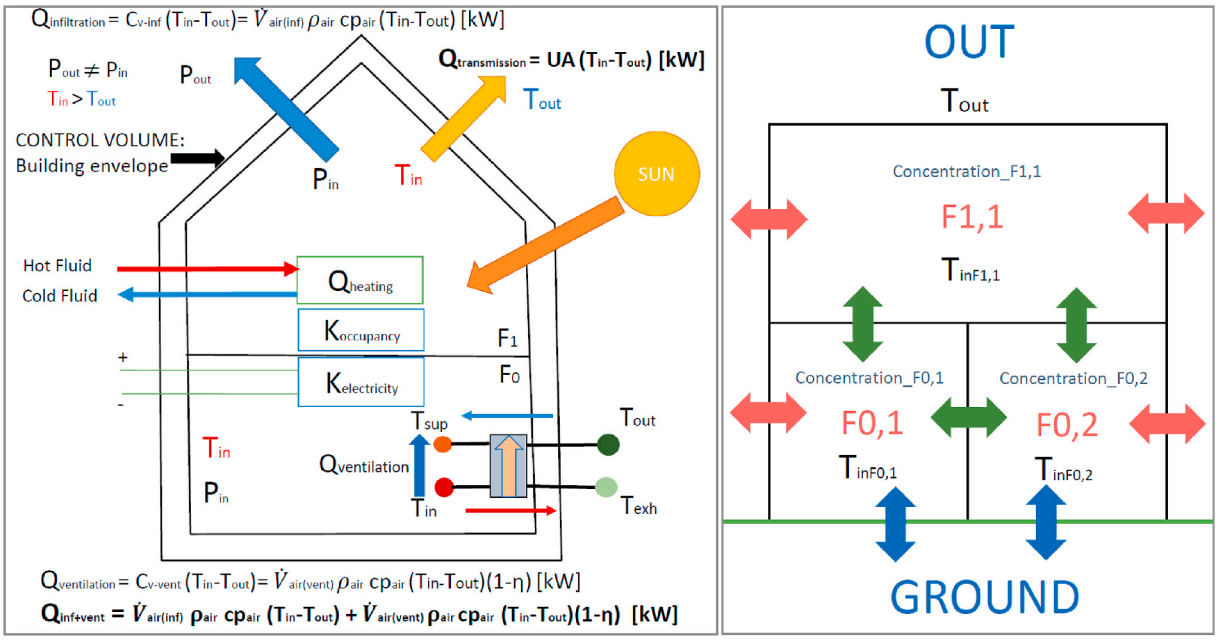

Fig. 3. LEFT: Schematic of all energy and mass exchanges through the control volume defined by the building envelope, including a schematic of a heat recovery system of a ventilation system of a building. RIGHT: Schematic of all energy and/or mass exchanges in a building composed of multiple thermal zones.

in Ref. [5]) allows to relate the HLC and the solar gains (S_aV_{sol}) to measurable variables. Those variables are the heating system energy supply (Q_k), all internal gains due to occupant metabolic heat generation and electrical devices consumption within the building envelope (K_k) and the $T_{in,k}$ to $T_{out,k}$ temperature difference present in Eq. (2), where *k* stands for an arbitrary measurement point. Building monitoring systems usually measure Eq. (2) measurable parameters (T_{in} and T_{out} [°C or K], Q [kW], K [kW] and V_{sol} [W/m^2]) in frequencies were Δt could range from 1 min to 1 h.

The average method obtains reliable HLC results, when Eq. (2) is applied during cold and cloudy winter short periods of 3–5 days and consequently, Q and ($T_{in} - T_{out}$) are high. Thus, their measurement uncertainty is minimum. On the other hand, in those cloudy periods where solar radiation is very low and could thus be considered purely diffuse, the uncertain in-use solar gains (S_aV_{sol}) are checked to be low compared to (Q + K). Thus, Eq. (2) can be reliably applied although solar gains are roughly estimated. The average method also requires to use periods with the same initial and final temperature level of the building, this way the energy accumulation term in the energy balance can be neglected.

$$HLC = \frac{\sum_{k=1}^{N}(Q_k + K_k + (S_aV_{sol})_k)}{\sum_{k=1}^{N}(T_{in,k} - T_{out,k})} \left[\text{kW/K}\right] \quad \text{Eq. (2)}$$

To develop the HLC decoupling methodology for buildings with multiple thermal zones, the properties of the HLC estimations related to multi thermal zones buildings are analysed. As shown previously, several heat gains and losses have been considered when estimating the HLC for a whole building enclosed in a control volume. However, the demonstration only considers the HLC estimation for a whole building with homogeneous indoor temperature (T_{in}). Eq. (3) to Eq. (13) (already presented in Ref. [5]) explain how different thermal zones next to each other, or on different storeys located above or under each other, behave when considering the whole building HLC. In other words, how the internal energy transfer effects passing from one room to another can be cancelled out through the analysis of the simple case of Fig. 3 (RIGHT) is proven. This figure shows a simple case for a multi thermal zone building that will be considered here a toy model. Three different volumes, distributed on two floors (F0 and F1), form the building. Each volume is affected by different internal gains and by heat and mass exchanges, coming either from other volumes, the ground or the exterior. Thus, we aim to prove that the building's total HLC can be estimated by applying the following formula:

$$HLC_{sum} = HLC_{F0,1} + HLC_{F0,2} + HLC_{F1,1} \ [\text{kW/K}] \quad \text{Eq. (3)}$$

where each thermal zone HLC can be estimated by applying Eq. (2) directly to each thermal zone as if they were only affected by ($T_{Fi,j} - T_{out}$). For clarity, the sum of Eq. (2) does not appear in the development until Eq. (13):

$$HLC_{F0,1} = \frac{\left[Q_{F0,1} + K_{F0,1} + (S_aV_{sol})_{F0,1}\right]}{\left(T_{F0,1} - T_{out}\right)} \ [\text{kW/K}] \quad \text{Eq. (4)}$$

$$HLC_{F0,2} = \frac{\left[Q_{F0,2} + K_{F0,2} + (S_aV_{sol})_{F0,2}\right]}{\left(T_{F0,2} - T_{out}\right)} \ [\text{kW/K}] \quad \text{Eq. (5)}$$

$$HLC_{F1,1} = \frac{\left[Q_{F1,1} + K_{F1,1} + (S_aV_{sol})_{F1,1}\right]}{\left(T_{F1,1} - T_{out}\right)} \ [\text{kW/K}] \quad \text{Eq. (6)}$$

In this example, two thermal zones are on the ground floor and another one on the first floor. Thus, the whole energy balance of each thermal zone (Eq. (7) to Eq. (9)) is presented considering all possible transmission and infiltration/ventilation exchanges for each of them:

Ground floor (volume $F_{0,1}$):

$$Q_{F0,1}+K_{F0,1}+(S_aV_{sol})_{F0,1}=UA_{F0,1-ground}(T_{F0,1}-T_{ground})+UA_{F0,1-F0,2}(T_{F0,1}-T_{F0,2})+UA_{F0,1-F1,1}(T_{F0,1}-T_{F1,1})+UA_{F0,1-out}(T_{F0,1}-T_{out})$$
$$+\dot{V}_{F0,1-F0,2}\rho_{air}Cp_{air}(T_{F0,1}-T_{F0,2})+\dot{V}_{F0,1-F1,1}\rho_{air}Cp_{air}(T_{F0,1}-T_{F1,1})+C_{vF0,1-out}(T_{F0,1}-T_{out})\ [\mathrm{kW}] \quad \text{Eq. (7)}$$

Ground floor (volume $F_{0,2}$):

$$Q_{F0,2}+K_{F0,2}+(S_aV_{sol})_{F0,2}=UA_{F0,2-ground}(T_{F0,2}-T_{ground})+UA_{F0,2-F0,1}(T_{F0,2}-T_{F0,1})+UA_{F0,2-F1,1}(T_{F0,2}-T_{F1,1})+UA_{F0,2-out}(T_{F0,2}-T_{out})$$
$$+\dot{V}_{F0,2-F0,1}\rho_{air}Cp_{air}(T_{F0,2}-T_{F0,1})+\dot{V}_{F0,2-F1,1}\rho_{air}Cp_{air}(T_{F0,2}-T_{F1,1})+C_{v\ F0,2-out}(T_{F0,2}-T_{out})\ [\mathrm{kW}] \quad \text{Eq. (8)}$$

First floor (volume $(F_{1,1})$):

$$Q_{F1,1}+K_{F1,1}+(S_aV_{sol})_{F1,1}=UA_{F1,1-F0,2}(T_{F1,1}-T_{F0,2})+UA_{F1,1-F0,1}(T_{F1,1}-T_{F0,1})+UA_{F1,1-out}(T_{F1,1}-T_{out})+\dot{V}_{F1,1-F0,2}\rho_{air}Cp_{air}(T_{F1,1}-T_{F0,2})$$
$$+\dot{V}_{F1,1-F0,1}\rho_{air}Cp_{air}(T_{F1,1}-T_{F0,1})+C_{vF1,1-out}(T_{F1,1}-T_{out})\ [\mathrm{kW}] \quad \text{Eq. (9)}$$

Since the average method considers periods with negligible energy accumulation within the building, when Eq. (7) to Eq. (9) are summed, all the energy transfers through internal walls due to transmission and infiltration between the considered thermal zones are cancelled out. Then, only heat and mass transfers between indoor and outdoor air and heat transfer between floor 0 volumes and ground remain.

$$HLC_{sum}=\frac{[Q_{F0,1}+K_{F0,1}+(S_aV_{sol})_{F0,1}]}{(T_{F0,1}-T_{out})}+\frac{[Q_{F0,2}+K_{F0,2}+(S_aV_{sol})_{F0,2}]}{(T_{F0,2}-T_{out})}+\frac{[Q_{F1,1}+K_{F1,1}+(S_aV_{sol})_{F1,1}]}{(T_{F1,1}-T_{out})}$$
$$=HLC_{F0,1}+HLC_{F0,2}+HLC_{F1,1}\ [\mathrm{kW/K}] \quad \text{Eq. (12)}$$

$$[Q_{F0,1}+K_{F0,1}+(S_aV_{sol})_{F0,1}]+[Q_{F0,2}+K_{F0,2}+(S_aV_{sol})_{F0,2}]+[Q_{F1,1}+K_{F1,1}+(S_aV_{sol})_{F1,1}]=UA_{F0,1-ground}(T_{F0,1}-T_{ground})+UA_{F0,1-out}(T_{F0,1}-T_{out})$$
$$+C_{v\ F0,1-out}(T_{F0,1}-T_{out})+UA_{F0,2-ground}(T_{F0,2}-T_{ground})+UA_{F0,2-out}(T_{F0,2}-T_{out})+C_{v\ F0,2-out}(T_{F0,2}-T_{out})+UA_{F1,1-out}(T_{F1,1}-T_{out})$$
$$+C_{v\ F1,1-out}(T_{F1,1}-T_{out})\ [\mathrm{kW}] \quad \text{Eq. (10)}$$

Since $HLC_{Fi,j}=UA_{Fi,j-out}+C_{v\ Fi,j-out}$ and taking $(T_{Fi,j}-T_{out})$ as the common factor for each volume and reordering, we obtain Eq. (11):

$$[Q_{F0,1}+K_{F0,1}+(S_aV_{sol})_{F0,1}]+[Q_{F0,2}+K_{F0,2}+(S_aV_{sol})_{F0,2}]+[Q_{F1,1}+K_{F1,1}+(S_aV_{sol})_{F1,1}]=HLC_{F0,1}(T_{F0,1}-T_{out})+HLC_{F0,2}(T_{F0,2}-T_{out})$$
$$+HLC_{F1,1}(T_{F1,1}-T_{out})\ [\mathrm{kW}] \quad \text{Eq. (11)}$$

Eq. (11) proves that the only valid solution for any $T_{Fi,j}$ is the one provided by Eq. (4) to Eq. (6) for each of the $HLC_{Fi,j}$ of Eq. (11), where each $HLC_{Fi,j}$ has only the indoor to outdoor $UA_{Fi,j-out}$ and $C_{v\ Fi,j-out}$ values within it. Remember that the $HLC_{F0,j}$ of the ground floor also includes the UA value against the ground multiplied by the factor $\frac{(T_{F0,j}-T_{ground})}{(T_{F0,j}-T_{out})}$. Thus, it has been proven that the whole building HLC can be estimated by the sum of the individual volumes $HLC_{Fi,j}$ as if they were only exchanging heat and mass with the outdoor air:

Generalizing this example to a building with L floors and M volumes per floor, Eq. (12) can be written as the general Eq. (13) (including de sum of Eq. (2)). Considering Eq. (2), it can be written as the sum of N time step measurements for the considered cold and cloudy period k = 1 (at t_1) to k = N (at t_2):

$$HLC_{sum}=\sum_{i=1}^{L}\sum_{j=1}^{M}HLC_{Fi,j}=\sum_{i=1}^{L}\sum_{j=1}^{M}\sum_{k=1}^{N}\frac{(Q_{i,j,k}+K_{i,j,k}+(S_aV_{sol})_{i,j,k})}{(T_{i,j,k}-T_{out,k})}\ [\mathrm{kW/K}] \quad \text{Eq. (13)}$$

From the previous analysis, it can be concluded that it is possible to develop a precise estimation of the whole building HLC estimating the HLCs for each thermal zone and summing them, since all the energy exchanges through the walls between the thermal zones are cancelled out when all the individual HLCs are summed. Moreover, it must be commented that there is no physical meaning when measuring the HLCs of each thermal zone independently, since this parameter includes the effect of the energy transmitted from one thermal zone to another. The individual HLCs of each thermal zone will only be physically meaningful when the same internal temperature is found in all the building's thermal zones. For this specific case, where all $T_{Fi,j}=T_{in}$, then Eq. (12) becomes Eq. (14):

$$HLC_{sum}=\frac{[Q_{F0,1}+K_{F0,1}+(S_aV_{sol})_{F0,1}]+[Q_{F0,2}+K_{F0,2}+(S_aV_{sol})_{F0,2}]+[Q_{F1,1}+K_{F1,1}+(S_aV_{sol})_{F1,1}]}{(T_{in}-T_{out})}=$$
$$HLC_{F0,1}+HLC_{F0,2}+HLC_{F1,1}\ [\mathrm{kW/K}] \quad \text{Eq. (14)}$$

This demonstration is crucial for the proposed HLC decoupling method feasibility since it gives a powerful tool to deal with the variations on internal temperature that might occur within a multi-storey occupied building where important temperature variations within the different building thermal zones are usual.

Now a similar development will be performed to prove that the building's total infiltration plus ventilation rates can be estimated by applying the following formula, where the Air Change per Hour (ACH) values of each thermal zone are obtained directly from the analysis of the decay curve of the anthropogenic CO_2 in each of those thermal zones:

$$\dot{V}_{building} = \dot{V}_{F0,1\_decay} + \dot{V}_{F0,2\_decay} + \dot{V}_{F1,1\_decay} \rightarrow \\ ACH_{building} V_{ol\_building} = ACH_{F0,1\_decay} V_{ol\_F0,1} + ACH_{F0,2\_decay} V_{ol\_F0,2} + ACH_{F1,1\_decay} V_{ol\_F1,1} \left[m^3/s\right] \quad \text{Eq. (15)}$$

To prove Eq. (15), it is necessary to start applying the mass balance to the three thermal zones represented in Fig. 3 (RIGHT). The accumulation of the mass within a building or a thermal zone within a building can be considered negligible. Otherwise, if even a small amount of air would be accumulated within a thermal zone of a building, its pressure would change considerably.

Ground floor (volume $F_{0,1}$):

$$0 = \left(\dot{m}_{out-F0,1} + \dot{m}_{F1,1-F0,1} + \dot{m}_{F0,2-F0,1}\right) - \left(\dot{m}_{F0,1-out} + \dot{m}_{F0,1-F0,2} + \dot{m}_{F0,1-F1,1}\right) \left[\text{kg/s}\right] \quad \text{Eq. (16)}$$

Ground floor (volume $F_{0,2}$):

$$0 = \left(\dot{m}_{out-F0,2} + \dot{m}_{F1,1-F0,2} + \dot{m}_{F0,1-F0,2}\right) - \left(\dot{m}_{F0,2-out} + \dot{m}_{F0,2-F0,1} + \dot{m}_{F0,2-F1,1}\right) \left[\text{kg/s}\right] \quad \text{Eq. (17)}$$

First floor (volume ($F_{1,1}$)):

$$0 = \left(\dot{m}_{out-F1,1} + \dot{m}_{F0,2-F1,1} + \dot{m}_{F0,1-F1,1}\right) - \left(\dot{m}_{F1,1-out} + \dot{m}_{F1,1-F0,1} + \dot{m}_{F1,1-F0,2}\right) \left[\text{kg/s}\right] \quad \text{Eq. (18)}$$

Furthermore, in the building sector, the pressure within the building and the temperature within the building is usually quite homogeneous regarding their possible effect on the variation of the density of the air within a building, thus the air density can be considered constant. Note that for the HLC estimation a 5 °C variation between thermal zones is an important variation since the indoor to outdoor temperatures used for HLC estimation usually range between 10 °C to 20 °C. Otherwise, a 5 °C variation on the air produces a negligible variation on its density. Then, since $\dot{m} = \dot{V}\rho_{air}$ and the density of the air (ρ_{air}) can be considered as a constant value, Eq. (16) to Eq. (18) are converted into:

$$0 = \left(\dot{V}_{out-F0,1} + \dot{V}_{F1,1-F0,1} + \dot{V}_{F0,2-F0,1}\right) - \left(\dot{V}_{F0,1-out} + \dot{V}_{F0,1-F0,2} + \dot{V}_{F0,1-F1,1}\right) \left[\text{m}^3/\text{s}\right] \quad \text{Eq. (19)}$$

$$0 = \left(\dot{V}_{out-F0,2} + \dot{V}_{F1,1-F0,2} + \dot{V}_{F0,1-F0,2}\right) - \left(\dot{V}_{F0,2-out} + \dot{V}_{F0,2-F0,1} + \dot{V}_{F0,2-F1,1}\right) \left[\text{m}^3/\text{s}\right] \quad \text{Eq. (20)}$$

$$0 = \left(\dot{V}_{out-F1,1} + \dot{V}_{F0,1-F1,1} + \dot{V}_{F0,2-F1,1}\right) - \left(\dot{V}_{F1,1-out} + \dot{V}_{F1,1-F0,2} + \dot{V}_{F1,1-F0,1}\right) \left[\text{m}^3/\text{s}\right] \quad \text{Eq. (21)}$$

Analysing Eq. (19) to Eq. (21), we can relate the total infiltration/ventilation rates of each thermal zone with its corresponding total ACH as follows:

$$ACH_{F0,1} V_{ol\_F0,1} = \dot{V}_{F0,1} = \left(\dot{V}_{out-F0,1} + \dot{V}_{F1,1-F0,1} + \dot{V}_{F0,2-F0,1}\right) = \left(\dot{V}_{F0,1-out} + \dot{V}_{F0,1-F0,2} + \dot{V}_{F0,1-F1,1}\right) \left[\text{m}^3/\text{s}\right] \quad \text{Eq. (22)}$$

$$ACH_{F0,2} V_{ol\_F0,2} = \dot{V}_{F0,2} = \left(\dot{V}_{out-F0,2} + \dot{V}_{F1,1-F0,2} + \dot{V}_{F0,1-F0,2}\right) = \left(\dot{V}_{F0,2-out} + \dot{V}_{F0,2-F0,1} + \dot{V}_{F0,2-F1,1}\right) \left[\text{m}^3/\text{s}\right] \quad \text{Eq. (23)}$$

$$ACH_{F1,1}V_{ol\_F1,1} = \dot{V}_{F1,1} = \left(\dot{V}_{out-F1,1} + \dot{V}_{F0,1-F1,1} + \dot{V}_{F0,2-F1,1}\right)$$
$$= \left(\dot{V}_{F1,1-out} + \dot{V}_{F1,1-F0,2} + \dot{V}_{F1,1-F0,1}\right) \left[m^3/s\right] \quad \text{Eq. (24)}$$

Applying the mass conservation principle (assuming (ρ_{air}) as a constant value) to the control volume enclosing the whole building we get:

$$0 = \left(\dot{V}_{out-F0,1} + \dot{V}_{out-F0,2} + \dot{V}_{out-F1,1}\right)$$
$$- \left(\dot{V}_{F0,1-out} + \dot{V}_{F0,2-out} + \dot{V}_{F1,1-out}\right) \left[m^3/s\right] \quad \text{Eq. (25)}$$

Making the sum Eq. (19) to Eq. (21), reordering and applying the equivalences of Eq. (22) to Eq. (26), the following expression is obtained:

$$ACH_{building}V_{ol\_building} = \left(\dot{V}_{out-F0,1} + \dot{V}_{out-F0,2} + \dot{V}_{out-F1,1}\right) = \left(\dot{V}_{F0,1-out} + \dot{V}_{F0,2-out} + \dot{V}_{F1,1-out}\right) \left[m^3/s\right] \quad \text{Eq. (26)}$$

the $ACH_{building}V_{ol\_building}$ of Eq. (27) are equal. For that, the following demonstration is done. As detailed in section 3.2, when applying the ASTM D6245-18 to a thermal zone of a building, the measured final concentration of CO_2 (C_F) of a thermal zone is related to the measured initial concentration (C_I) and to the ACH_{decay} with the following formula:

$$C_F = C_I e^{-ACH_{decay}\,t}\left[ppm_{CO2}, \frac{mol_{CO2}}{mol_{air}}, \frac{m^3_{CO2}}{m^3_{air}}\right] \quad \text{Eq. (28)}$$

If there are mass interactions between thermal zones with different CO_2 concentrations together with mass interactions with the outdoors ambient, the ACH_{decay} will be different to the ACH values as calculated in Eq. (22) to Eq. (24). However, when the mass balance of CO_2 is done for the whole building of Fig. 3 (RIGHT) during a decay analysis period between t = 0 [s] to t = t [s], we get the following equation:

$$\left(C_{IF0,1} - C_{FF0,1}\right)V_{ol.F0,1}\rho_{CO2} + \left(C_{IF0,2} - C_{FF0,2}\right)V_{ol.F0,2}\rho_{CO2} + \left(C_{IF1,1} - C_{FF1,1}\right)V_{ol.F1,1}\rho_{CO2} = \left(\frac{n_{CO2,I,building}}{n_{air}} - \frac{n_{CO2,F,building}}{n_{air}}\right)V_{ol.building}\rho_{CO2}$$
$$= \left(C_{I\,building} - C_{F\,building}\right)V_{ol,building}\rho_{CO2}\,[kg]$$
$$\left(C_{IF0,1} - C_{FF0,1}\right)V_{ol.F0,1} + \left(C_{IF0,2} - C_{FF0,2}\right)V_{ol.F0,2} + \left(C_{IF1,1} - C_{FF1,1}\right)V_{ol.F1,1} = \left(\frac{n_{CO2,I,building}}{n_{air}} - \frac{n_{CO2,F,building}}{n_{air}}\right)V_{ol.building} = \left(C_{I\,building} - C_{F\,building}\right)V_{ol.building}\left[m^3\right] \quad \text{Eq. (29)}$$

$$ACH_{building}V_{ol\_building} = ACH_{F0,1}V_{ol\_F0,1} + ACH_{F0,2}V_{ol\_F0,2} + ACH_{F1,1}V_{ol\_F1,1}\left[m^3/s\right] \quad \text{Eq. (27)}$$

Unless the thermal zones within a building are completely airtight between them, the $ACH_{F0,1\_decay}$ of Eq. (15) will not be equal to the $ACH_{F0,1}$ of Eq. (27). However, the application of the HLC decoupling method only requires to prove that the $ACH_{building}V_{ol\_building}$ of Eq. (15) and

Note that assuming Amagat Model [35] using the molar fraction or the volume fraction is equivalent to express the concentration. The Amagat Model assumes that the total volume of a mixture of ideal gases, is the sum of the partial volumes of each of the components of the mixture as if they were at the same total pressure and temperature as the mixture. Those partial volumes are proportional to the molar fraction its species has in the gas mixture. Assuming the total volume is the building volume and that the building indoor air total pressure and temperature have small variations regarding the density calculation of each of those

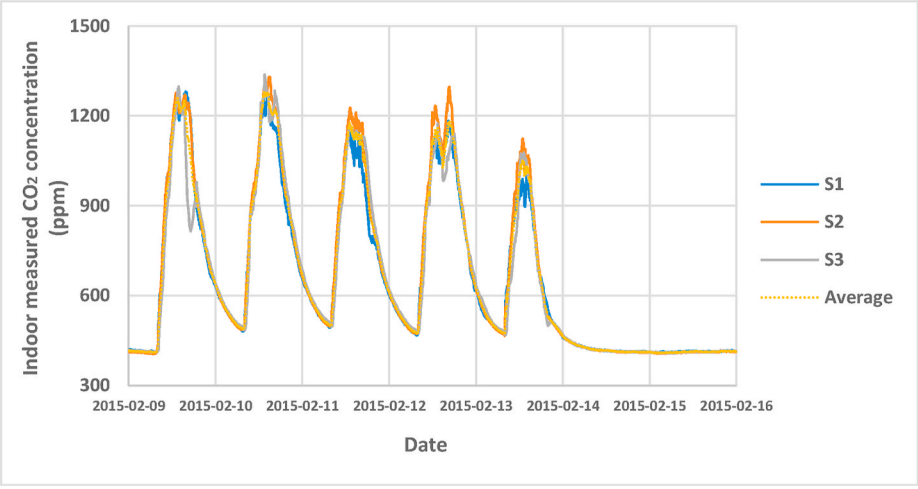

Fig. 4. Minute by minute measured air quality data of each sensor of F1 from 9th to February 15, 2015 over time.

partial volumes, the CO_2 density associated to the partial volume occupied by the CO_2 at the beginning of the decay period analysis and at the end of the decay period analysis can be considered constant. Thus, the mass balance, the molar balance and the volume balance of the CO_2 are equivalent in Eq. (29). This is a valid model when the working gas behaves as an ideal gas, and the air, in usual building indoor conditions, behaves as an ideal gas. In Eq. (29) $n_{CO2.I.building}$ and $n_{CO2.F.building}$ are the total number of moles of CO_2 within the whole building at t = 0 [s] and at t = t [s], respectively. While n_{air} are the total number of moles of air within the whole building (it can be considered constant during the decay method application period unless huge temperature and/or pressure variations occur within the building). Thus, the term $(C_{Ibuilding} - C_{Fbuilding})V_{ol\_building}$ represents the net amount of CO_2 that has been transferred from the building to the exterior during the decay period.

The decay method only considers the measured $C_{IFi,j}$ and the measured $C_{FFi,j}$ to estimate the corresponding thermal zone ACH_{Fi,j_decay}. Obviously, unless the thermal zones are completely airtight between them, the ACH_{Fi,j_decay} in general will be different to the $ACH_{Fi,j}$ calculated as in Eq. (22) to Eq. (24). For example, if F0,1 has the same indoor concentration as F0,2, even if there are infiltration exchanges between F0,1 and F0,2, the decrease on the concentration of F0,1, will only be due to the mass exchange of the F0,1 with the outdoors air. Then, in this case, even if the $ACH_{Fi,j}$ considers both mass exchanges (with the outdoor air and with F0,2), the decay analysis will only identify the part of the mass exchange that generates a concentration variation, this is, the exchange with the outdoors represented by ACH_{Fi,j_decay}.

Including Eq. (28) into Eq. (29) the following expression is obtained:

$$\begin{aligned}&\left(C_{IF0,1} - C_{IF0,1}e^{-ACH_{F0,1\_decay}\ t}\right)V_{ol\_F0,1} + \left(C_{IF0,2} - C_{IF0,2}e^{-ACH_{F0,2\_decay}\ t}\right)V_{ol\_F0,2}\\ &+ \left(C_{IF1,1} - C_{IF1,1}e^{-ACH_{F1,1\_decay}\ t}\right)V_{ol\_F1,1}\\ &= \left(C_{Ibuilding} - C_{Ibuilding}e^{-ACH_{building}\ t}\right)V_{ol\_building}\ \left[m^3\right]\end{aligned}$$

Eq. (30)

Since Eq. (30) fulfils the net CO_2 mass balance during a decay analysis test for the whole building, Eq. (15) must also fulfil the air balance on the whole building basis. Of course, when the infiltration exchanges between thermal zones tend to zero, the individual ACH_{Fi,j_decay} values of Eq. (15) will tend to be equal to the $ACH_{Fi,j}$ of Eq. (27).

Resuming, when all the thermal zones of a building have the same indoor air temperature, if the HLC of those thermal zones is estimated, they will represent the HLC value of those thermal zones regarding the outdoors air. Thus they will be meaningful in the sense that they do not consider energy exchanges with other thermal zones within the building. If the thermal zones have different temperatures, then the individual HLCs of the thermal zones will not represent the HLC of those thermal zones with the outdoors air. But even if individually they are not meaningful, when we aggregate all the HLCs of all the thermal zones, they represent the total HLC of the whole building envelope.

On the other hand, when the infiltration plus ventilation mass flow rates are estimated by means of the ACH_{decay} values obtained by means of the anthropogenic CO_2 decay analysis, they will only represent the total air flow exchange of the analysed thermal zone when the occupied thermal zones are completely airtight between them. In those cases, they will represent the mass exchange with the outdoors. However, if we sum all the infiltration plus ventilation rates of all the thermal zones of a building estimated by means of the ACH_{decay} values, the total building infiltration plus ventilation rates with the outdoors are obtained even if the thermal zones are not airtight between them.

In other words, only when all the building thermal zones have the same indoor air temperature and are completely airtight between them, the individual HLCs have physical meaning and could be decoupled maintaining the physical meaning with the estimated ACH_{decay} values.

Nevertheless, as shown in the results of [5], due to the similarity of the measured indoor temperatures in the different floors of the analysed four storey office building, the obtained individual thermal zones HLC results are meaningful. Furthermore, the thermal zones considered in the analysed building are separated by continuous concrete slabs, thus, the considered thermal zones are assumed to be airtight between them.

After the above demonstration, in order to develop further the method for the HLC estimation presented in Ref. [5], the next section describes the metabolic CO_2 decay method applied to estimate the thermal zone's Air Change per Hour (ACH_{decay}) and then the infiltration heat loss coefficient estimation method ($C_{v\text{-}inf}$). Since only the infiltration heat loss coefficient is estimated in this work, from now, it is called C_v. Finally, considering the HLC estimated previously, and the C_v estimated during this study, the decoupling method used is also described in detail.

3.2. Air change per hour (ACH_{decay}) estimation method

The metabolic CO_2 of the building's occupants has been used as tracer gas to estimate air infiltration rates by means of CO_2 concentration decay analysis. The concentration decay method is well explained in Ref. [36].

The use of CO_2 generated from occupants as a tracer gas to determine air change rates in buildings is described in ASTM D6245-18, the 'Standard Guide for Using Indoor Carbon Dioxide Concentrations to Evaluate Indoor Air Quality and Ventilation' [33]. According to this guide, and together with the ASTM E741-11 Method [34], air change rates (or Air Changes per Hour, ACH_{decay} in $[h^{-1}]$) can be estimated using the tracer gas decay technique in which occupant-generated CO_2 is used as a tracer gas if the measurements are conducted after the occupants leave the building.

These are the requirements established by the ASTM D6245-18 guide affecting this work:

- Section 9.3.1 of the guide: The decay technique is based on the assumption that there is no source of tracer gas in the building, which in the case of CO_2 means that the building is no longer occupied. In practice, an occupancy density of one person per 1000 m^2 or less will not impact the measurement results. To fulfil this requirement, data from 18:00 to 20:00 h has been used, shortly after the end of the working day.
- Section 9.3.2.: The tracer gas decay technique, as described in the Test Method ASTM E741-11, assumes that the outdoor tracer gas concentration is zero, which is not the case with CO_2. However, if the outdoor concentration is constant during the decay measurement, then the tracer gas decay technique can be used by substituting the difference between the indoor and outdoor concentrations for the indoor concentration in the analysis contained in the Test Method. Analysing the data sets and having Fig. 4 as an example, it can be stated that the background CO_2 concentration changes very little. The variation is within 3–5 ppm (minimum individual measurement 395 ppm), thus the background or outdoor concentration is considered constant as 400 ppm.
- Section 9.3.3.: The concentration measurement uncertainty must be better than ±5 % during the decay analysis period. When using CO_2 as a tracer gas, this precision requirement must be applied to the difference between the indoor to outdoor CO_2 concentrations. As shown in the experimental set-up section of this paper, the monitoring system used in this study fulfils this requirement if the 350 ppm condition established in section 9.3.4 is fulfilled.
- Section 9.3.4.: The indoor CO_2 concentration when the building is finally unoccupied depends on the concentration in the building when the occupants start leaving, the amount of time it takes them to leave, and the air change rate of the building. Depending on the values of these parameters, the indoor CO_2 concentration may be too low once the building is unoccupied to perform a reliable tracer gas decay measurement. These authors propose an initial minimum

acceptable value of the decay should be 350 ppm (the difference between the indoor and outdoor concentrations) to avoid low concentration values at the end of the measurements that could reduce the reliability of the measurements. This minimum initial value permits section 9.3.3 uncertainty requirement to be fulfilled at the end of all the periods analysed in this work. This minimum value has been fixed following a procedure that permits the ±5 % accuracy stated in section 9.3.3 to be complied with, even at the end of the decay curve. The previously mentioned Eq. (28), now named as Eq. (31), can be used to estimate the final indoor to outdoor concentration difference:

$$C_F = C_I e^{-ACH_{decay}\ t}\left[ppm_{CO2}, \frac{mol_{CO2}}{mol_{air}}, \frac{m^3_{CO2}}{m^3_{air}}\right] \quad \text{Eq. (31)}$$

where C_F is the final indoor to outdoor concentration difference [ppm], C_I is the initial indoor to outdoor concentration difference [ppm] (350 ppm is assumed to be the initial minimum possible value), ACH_{decay} is the Air Change per Hour [h^{-1}] and t is the time [h] (2 h in our analysis). Then, fixing the initial minimum indoor to outdoor concentration difference (C_I) and considering the maximum ACH_{decay} value obtained for all the identified valid days for analysis, it is possible to check whether the selected C_I value is high enough to fulfil the 9.3.3 uncertainty requirement for all the estimated C_F values. Therefore, Eq. (32) is used to check if the lowest estimated C_F value provided by Eq. (31) fulfils the ±5 % accuracy stated in section 9.3.3:

$$Relative\ error = \frac{Total\ measurement\ error}{C_F} \times 100 = < 5\ \% \quad \text{Eq. (32)}$$

where the "Total measurement error" is the ((C_F + 400 ppm) x error

Table 3
Data for the calculation of ACH_{decay} values that fulfil the ASTM requirements in February 2015 for the first floor. Note that the initial and final values of the concentrations show the difference between the indoor to outdoor concentrations.

		Initial CO_2 concentration (ppm)				Difference from the average (%)			Final CO_2 concentration (ppm)				Difference from the average (%)		
Day	ACH decay	Aver.	S1 1.2.4	S2 1.2.6	S3 1.2.8	S1 1.2.4	S2 1.2.6	S3 1.2.8	Aver.	S1 1.2.4	S2 1.2.6	S3 1.2.8	S1 1.2.4	S2 1.2.6	S3 1.2.8
1	-0.07	9.2	10.0	7.0	10.5	9.1	-23.6	14.5	9.0	8.0	7.0	12.0	-11.1	-22.2	33.3
2	**0.19**	**704.7**	**669.0**	**706.0**	**739.0**	**-5.1**	**0.2**	**4.9**	**485.7**	**466.0**	**477.0**	**514.0**	**-4.0**	**-1.8**	**5.8**
3	0.20	701.3	648.0	653.0	803.0	-7.6	-6.9	14.5	479.7	452.0	458.0	529.0	-5.8	-4.5	10.3
4	0.59	355.3	372.0	336.0	358.0	4.7	-5.4	0.8	98.7	104.0	83.0	109.0	5.4	-15.9	10.5
5	0.41	263.0	264.0	257.0	268.0	0.4	-2.3	1.9	127.7	146.0	107.0	130.0	14.4	-16.2	1.8
6	**0.28**	**424.3**	**419.0**	**420.0**	**434.0**	**-1.3**	**-1.0**	**2.3**	**246.8**	**257.0**	**239.0**	**244.5**	**4.1**	**-3.2**	**-0.9**
7	0.00	27.8	30.5	24.0	29.0	9.6	-13.8	4.2	27.3	28.0	24.0	30.0	2.4	-12.2	9.8
8	0.03	17.7	20.0	14.0	19.0	13.2	-20.8	7.5	17.3	19.0	14.0	19.0	9.6	-19.2	9.6
9	0.12	564.0	598.0	608.0	486.0	6.0	7.8	-13.8	443.8	425.0	442.5	464.0	-4.2	-0.3	4.5
10	**0.15**	**694.3**	**635.0**	**710.0**	**738.0**	**-8.5**	**2.3**	**6.3**	**507.7**	**464.0**	**527.0**	**532.0**	**-8.6**	**3.8**	**4.8**
11	0.15	561.0	477.0	563.0	643.0	-15.0	0.4	14.6	403.0	376.0	404.0	429.0	-6.7	0.2	6.5
12	**0.18**	**712.3**	**674.0**	**724.0**	**739.0**	**-5.4**	**1.6**	**3.7**	**503.7**	**493.0**	**512.0**	**506.0**	**-2.1**	**1.7**	**0.5**
13	0.36	247.3	260.0	245.0	237.0	5.1	-0.9	-4.2	127.0	150.0	130.0	101.0	18.1	2.4	-20.5
14	-0.01	12.7	13.0	11.0	14.0	2.6	-13.2	10.5	12.0	13.0	11.0	12.0	8.3	-8.3	0.0
15	-0.05	12.2	11.0	11.0	14.5	-9.6	-9.6	19.2	14.7	16.0	14.0	14.0	9.1	-4.5	-4.5
16	0.71	471.2	500.0	484.5	429.0	6.1	2.8	-8.9	116.3	171.0	113.0	65.0	47.0	-2.9	-44.1
17	0.34	224.0	246.0	217.0	209.0	9.8	-3.1	-6.7	114.7	127.0	114.0	103.0	10.8	-0.6	-10.2
18	**0.18**	**614.0**	**604.0**	**642.0**	**596.0**	**-1.6**	**4.6**	**-2.9**	**436.0**	**436.0**	**450.0**	**422.0**	**0.0**	**3.2**	**-3.2**
19	**0.20**	**511.7**	**532.0**	**511.0**	**492.0**	**4.0**	**-0.1**	**-3.8**	**346.7**	**333.0**	**355.0**	**352.0**	**-3.9**	**2.4**	**1.5**
20	**0.19**	**366.3**	**342.0**	**388.0**	**369.0**	**-6.6**	**5.9**	**0.7**	**253.0**	**239.0**	**259.0**	**261.0**	**-5.5**	**2.4**	**3.2**
21	-0.04	4.3	4.0	3.0	6.0	-7.7	-30.8	38.5	4.0	5.0	1.0	6.0	25.0	-75.0	50.0
22	-0.35	0.3	2.0	-1.0	0.0	500.0	-400.0	-100.0	0.7	1.0	1.0	0.0	50.0	50.0	-100.0
23	0.41	315.0	413.0	370.0	162.0	31.1	17.5	-48.6	142.0	169.0	170.0	87.0	19.0	19.7	-38.7
24	0.71	214.3	264.0	229.0	150.0	23.2	6.8	-30.0	61.7	79.0	57.0	49.0	28.1	-7.6	-20.5
25	0.56	138.3	169.0	142.0	104.0	22.2	2.7	-24.8	46.2	55.5	45.0	38.0	20.2	-2.5	-17.7
26	0.47	449.0	474.0	483.0	390.0	5.6	7.6	-13.1	178.3	241.0	203.0	91.0	35.1	13.8	-49.0
27	0.27	107.7	135.0	111.0	77.0	25.4	3.1	-28.5	63.3	78.0	60.0	52.0	23.2	-5.3	-17.9
28	-0.07	11.0	12.0	10.0	11.0	9.1	-9.1	0.0	12.0	14.0	10.0	12.0	16.7	-16.7	0.0

Table 4
The rest of the ACH_{decay} results, regression equations and R^2 values of February 2015 fulfilling the ASTM D6245-18 requirements for the first floor.

Day	ACH_{decay}	Regression equation	R^2
10	0.15	y = −0.1514x+9.2406	0.9858
12	0.18	y = −0.1770x+9.7566	0.9962
18	0.18	y = −0.1775x+9.6071	0.9924
19	0.20	y = −0.1952x+9.7323	0.9845
20	0.19	y = −0.1894x+9.3324	0.9877

of the sensor (1 % in this case)). Then, if this lowest possible C_F is lower than 5 %, it would be possible to fulfil section 9.3.3 uncertainty requirement for all the measurements carried out in this work. Then, the selected minimum of 350 ppm for the C_I value would be a proper initial indoor to outdoor concentration difference for all cases.

- Section 9.3.5.: The Test Method ASTM E741-11 requires that the indoor tracer gas concentration at multiple points (at least three) within the analysed thermal zone (a floor in this case) differs by less than 10 % of the average concentration in the floor (at least at the beginning and end of the sampling period). When using CO_2, this concentration uniformity requirement should be applied to the difference between the indoor to outdoor concentrations.

Due to the different spatial distributions of F0 and F2, the last requirement has never been fulfilled for these two floors for any of the days of the analysed period (December 2014 to March 2016). Since these floors are formed by smaller office rooms, it is impossible to homogenise the CO_2 in the whole floor. Therefore, for these two floors, the last requirement has been substituted by the following proposed extra-requirement to ensure acceptable results for some days of the analysed period:

- To ensure no windows are opened, the maximum acceptable value of outdoor daily average temperature has been established at 10 °C, assuming the building's users will not open windows with such low outdoor temperatures. In fact, the not opening of windows is only required for the period 18:00 to 20:00, when the decay analysis is applied. If a window is opened, for example from 16:00 to 17:00, there will be a sudden drop of the CO_2 and it will make it more difficult to fulfil the 9.3.4 and 9.3.5 criteria in the subsequent period 18:00 to 20:00. In this work, the decay analysis has been done manually for each of the daily regressions. The opening of windows has been detected visually in the monitored data by representing the CO_2 ppm over time, as in Fig. 4, where the sensor 'S3' has a sudden drop from 16:00 to 17:30 on the first day (9th February). This is a clear window opening of the office where the sensor 'S3' is installed. If this type of disturbance were present in any of the floor sensors between 18:00 to 20:00, the data of the corresponding day would have been discarded. In any case, on cold days, the opening of windows was not detected after 18:00. It is thus possible to ensure similar window opening behaviour in all the different compartmentalised offices. Thus, measuring only CO_2 concentrations in a few of them would be sufficient, since the infiltration behaviour can be assumed to be similar for all of them. On hotter days, it is possible to have different window opening behaviours between compartmentalised offices and, thus, measuring CO_2 in a few of them will lead to erroneous results. Although this time the window opening check has been done visually, it seems feasible to be able to automatically detect window openings by analysing the CO_2 concentrations over time, as discussed above.

The Air Changes per Hour (ACH_{decay} in [h^{-1}]) of each day fulfilling the above requirements have been estimated for each floor, using the available minute CO_2 concentration data in [ppm]. The average

Table 5
The daily ACH_{decay} and average wind speed (WS [m/s]) values of all days fulfilling ASTM requirements for F1 and F3. The last row presents the average ACH_{decay_aver} values for F1 and F3 for the selected period (December 2014–March 2015). 95 % confidence intervals are presented for the averaged values using the t-student distribution.

FLOOR 1			FLOOR 3		
DATE	ACH_{decay}	WS [m/s]	DATE	ACH_{decay}	WS [m/s]
4-12-2014	0.19	0.59	2-12-2014	0.19	0.54
11-12-2014	0.18	0.58	4-12-2014	0.29	0.59
15-12-2014	0.23	0.30	9-12-2014	0.19	0.70
8-1-2015	0.24	0.34	15-12-2014	0.19	0.30
9-1-2015	0.21	0.55	18-12-2014	0.25	1.75
12-1-2015	0.20	3.86	5-1-2015	0.17	0.33
15-1-2015	0.23	1.45	7-1-2015	0.16	0.50
2-2-2015	0.19	1.01	8-1-2015	0.22	0.34
6-2-2015	0.28	2.57	9-1-2015	0.20	0.55
10-2-2015	0.15	0.75	12-1-2015	0.21	3.86
12-2-2015	0.18	0.94	13-1-2015	0.19	1.65
18-2-2015	0.18	0.50	15-1-2015	0.16	1.45
19-2-2015	0.20	0.41	19-1-2015	0.20	1.81
20-2-2015	0.19	3.83	22-1-2015	0.30	2.54
2-3-2015	0.13	1.25	23-1-2015	0.19	0.30
5-3-2015	0.19	1.36	26-1-2015	0.16	1.76
-	-	-	27-1-2015	0.23	1.72
-	-	-	2-2-2015	0.24	1.01
-	-	-	6-2-2015	0.24	2.57
-	-	-	10-2-2015	0.17	0.75
-	-	-	11-2-2015	0.20	2.40
-	-	-	12-2-2015	0.16	0.94
-	-	-	17-2-2015	0.27	4.02
-	-	-	2-3-2015	0.19	1.25
-	-	-	3-3-2015	0.11	0.18
-	-	-	11-3-2015	0.18	0.42
-	-	-	16-3-2015	0.25	2.83
-	-	-	23-3-2015	0.34	1.37
AVERAGE	**0.20 ± 0.018 (ACH_{decay_aver})**	-	**AVERAGE**	**0.21 ± 0.019 (ACH_{decay_aver})**	-

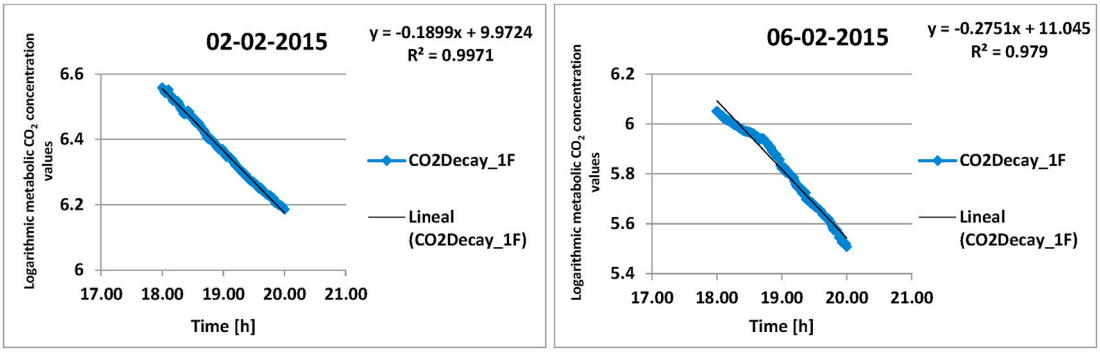

Fig. 5. Two examples of the ACH_{decay} values obtained by linear regression for February 2015 fulfilling all ASTM D6245-18 requirements for the first floor. y-axis: Logarithmic metabolic CO_2 concentration values [LN (measured indoor CO_2 ppm - outdoors 400 CO_2 ppm)]; x-axis: time in [h].

ACH_{decay_aver} of each floor for each considered winter period is therefore the average of the ACH_{decay} values for those days that meet all the above requirements within the analysed winter. Then, for each analysed winter period, the ACH_{decay_aver} of each floor is used for the estimation of the floor-by-floor infiltration heat loss coefficient (C_v).

3.3. Air infiltration heat loss coefficient (C_v) estimation

When analysing the data of the two considered winters, no ventilation heat losses need to be considered, since there was no ventilation system installed in the building during these winter periods. Then, based on the ACH_{decay} values estimated using section 3.2 methodology, it is possible to estimate the air infiltration heat loss coefficient ((C_v) in [kW/K]) of each analysed floor using Eq. (33).

$$C_v = V_{ol\_floor} ACH_{decay\_aver} \rho_{air} Cp_{air} \text{ [kW/K]} \quad \text{Eq. (33)}$$

where V_{ol_floor} is the volume of each floor [m^3], ACH_{decay_aver} is the floor average Air Change per Hour for the whole considered testing period in [h^{-1}], ρ_{air} [kg/m^3] and Cp_{air} [kJ/kg°C] are the density and the constant pressure specific heat of the air at the average indoor temperature, respectively. Note that, in this equation, it is necessary to convert ACH_{decay_aver} to [s^{-1}] to obtain the C_v in [kW/K].

For the ground and second floors, an extra calculation has been made to guarantee appropriate results. Taking into account the distribution of these two floors and the location of the air quality sensors, each sensor has been assigned a portion of the total volume of each floor (see Fig. 2), and the C_v of the ground floor and second floor have been estimated using both Eq. (33) and Eq. (34). The results obtained by Eq. (33) and Eq. (34) have then been compared.

$$C_v = \sum_{i=1}^{N} \left(V_{ol\_i} \times ACH_{decay\_aver\_Vi}\right) \rho_{air} Cp_{air} \text{ [kW/K]} \quad \text{Eq. (34)}$$

where V_{ol_i} and $ACH_{decay\_aver\_Vi}$ are the volume portions and the average Air Change per Hour of the considered period associated with each volume portion, respectively, and N is the number of divisions made in the total volume of each floor (see Fig. 2).

3.4. Estimation of the transmission heat loss coefficient (UA)

Sections 3.2 and 3.3 have already described the method used, based on the ASTM D6245-18 guide, to estimate the infiltration heat loss coefficient. However, in order to achieve the aim of this work, it is necessary to use these results together with the previously estimated HLC values in Ref. [5] to estimate the transmission heat loss coefficient. Thus, it would be possible to know which of the coefficients, the transmission heat loss coefficient or the infiltration heat loss coefficient, is the main responsible factor for the energy losses regarding the building envelope. Therefore, the average floor-by-floor infiltration heat loss coefficient value for each of the winters is subtracted from each floor HLC value of the corresponding winter. The same is done with the sum of all the floors in order to estimate the total results for the whole building. This procedure is carried out using Eq. (35).

$$UA = HLC - C_v \text{ [kW/K]} \quad \text{Eq. (35)}$$

4. Results and discussion

The analysis has been carried out using data provided from the monitored in-use building between November 2014 and March 2017. Three individual winter periods can be found, 2014–2015, 2015–2016 and 2016–2017, before the rehabilitation of the building. Unfortunately, due to the lack of data concerning monitoring problems, it has been impossible to analyse the winter 2016–2017. So, the minute by minute air quality data (CO_2 ppm) from December 2014 to March 2016 of the metabolic CO_2 of the building's occupants is used to estimate air infiltration rates by means of the CO_2 concentration decay analysis presented above.

Plotting and applying the linear regression to the tracer gas (in this case the indoor to outdoor CO_2 concentration in ppm) concentration decay over time in [h] (from 18:00 h to 20:00 h) on a natural logarithmic basis, the Air Change per Hour rates (ACH_{decay}) of each floor have been calculated for every day of the abovementioned period. Then, only the ACH_{decay} values of those days that fulfil the aforementioned requirements have been taken into consideration for the C_v estimation. Finally, for each winter period, the floor-by-floor estimated C_v values have been subtracted from the HLC estimates of each corresponding winter period to estimate each floor-by-floor transmission heat loss coefficient.

4.1. Air change per hour (ACH_{decay}) calculation

In Fig. 4, the air quality data for each sensor has been plotted for F1 from 9th to February 15, 2015. In the example shown in Fig. 4, the charging and discharging periods of CO_2 concentration can be clearly seen, with an exponential discharge coinciding with the end of the working day (about 17:00). This exponential discharge resembles a straight line when plotted on a logarithmic basis.

Table 3 shows an example of the calculations for the whole month of February 2015 for the first floor (F1). Non-working days (red lines) have very low indoor to outdoor concentrations because the building is empty from Friday afternoon until Monday morning. Thus, by Saturday 18:00 h, there are already very similar CO_2 concentrations to the outdoor one and both the indoor to outdoor initial and final concentration values are very low and similar to each other. Of course, none of those non-working days fulfil the ASTM D6245-18 requirements and so are not considered in Table 5 for the latter C_v estimations. Those days where the CO_2 concentration at any of the sensors (S1, S2 or S3, see Table 3 and Fig. 2 for sensor codes) within the floor differs by more than 10 % of the

Table 6
ACH_{decay} values of each volume portion and average wind speed (WS [m/s]) of F0 and F2, and the average ACH_{decay} values associated to each whole floor for the selected period (December 2014–March 2015). 95 % confidence intervals are presented for the averaged values using the t-student distribution.

DATE	T_{out}	FLOOR 0				FLOOR 2					WS [m/s]
		ACH $_{decay\_V1}$	ACH $_{decay\_V2}$	ACH $_{decay\_V3}$	Daily ACH_{decay} average	ACH $_{decay\_V1}$	ACH $_{decay\_V2}$	ACH $_{decay\_V3}$	ACH $_{decay\_V4}$	Daily ACH_{decay} average	
3-12-2014	8.88	–	–	–	–	0.04	0.06	0.29	0.37	0.20	0.44
4-12-2014	8.65	0.06	0.07	0.46	0.25	0.09	0.06	0.19	0.25	0.13	0.59
5-12-2014	8.35	0.26	0.31	0.47	0.37	–	–	–	–	–	3.22
9-12-2014	9.38	0.06	0.11	0.41	0.25	0.07	0.08	0.25	0.18	0.13	0.70
15-12-2014	10.06	–	–	–	–	0.08	0.08	0.21	0.24	0.11	0.30
7-1-2015	9.26	0.23	0.19	0.36	0.25	0.05	0.07	0.13	0.14	0.09	0.50
8-1-2015	9.65	0.21	0.30	0.40	0.29	0.06	0.06	0.07	0.03	0.06	0.34
20-1-2015	6.19	0.25	0.20	0.33	0.25	0.09	0.10	0.20	0.07	0.11	0.70
22-1-2015	6.56	0.14	0.34	0.59	0.43	0.13	0.09	0.24	0.22	0.16	2.54
23-1-2015	6.78	0.11	0.15	0.36	0.21	–	–	–	–	–	0.30
26-1-2015	7.92	0.08	0.07	0.40	0.21	0.08	0.09	0.14	0.10	0.09	1.76
27-1-2015	9.13	0.24	0.15	0.47	0.33	0.11	0.10	0.23	0.26	0.15	1.72
30-1-2015	8.88	0.12	0.10	0.33	0.19	–	–	–	–	–	0.92
2-2-2015	6.55	0.16	0.15	0.25	0.19	0.12	0.10	0.14	0.06	0.10	1.01
3-2-2015	4.49	–	–	–	–	0.12	0.09	0.25	0.13	0.13	4.23
6-2-2015	1.51	0.19	0.16	0.42	0.29	–	–	–	–	–	2.57
10-2-2015	6.33	0.25	0.27	0.39	0.29	0.08	0.08	0.19	0.07	0.09	0.75
17-2-2015	8.78	–	–	–	–	0.15	0.13	0.20	0.23	0.17	4.02
18-2-2015	8.30	–	–	–	–	0.09	0.06	0.32	0.17	0.13	0.50
19-2-2015	8.32	–	–	–	–	0.06	0.08	0.28	0.33	0.16	0.41
5-3-2015	8.84	–	–	–	–	0.02	0.04	0.09	0.17	0.08	1.36
16-3-2015	8.71	0.33	0.28	0.41	0.33	0.06	0.07	0.09	0.17	0.09	2.83
23-3-2015	6.38	–	–	–	–	0.12	0.06	0.29	0.36	0.16	1.37
24-3-2015	7.71	–	–	–	–	0.19	0.18	0.48	0.21	0.22	3.05
Average	**-**	**0.18 ± 0.046 (ACH $_{decay\_aver\_V1}$)**	**0.19 ± 0.050 (ACH $_{decay\_aver\_V2}$)**	**0.40 ± 0.043 (ACH $_{decay\_aver\_V3}$)**	**0.28 ± 0.038 (ACH $_{decay\_aver}$)**	**0.09 ± 0.019 (ACH $_{decay\_aver\_V1}$)**	**0.08 ± 0.014 (ACH $_{decay\_aver\_V2}$)**	**0.21 ± 0.045 (ACH $_{decay\_aver\_V3}$)**	**0.19 ± 0.046 (ACH $_{decay\_aver\_V4}$)**	**0.13 ± 0.019 (ACH $_{decay\_aver}$)**	**-**

Table 7
The daily C_v values estimated for all the floors. The last row presents the average C_{v_aver} values for all floors for the selected period (December 2014–March 2015). 95 % confidence intervals are presented for the averaged values using the t-student distribution.

FLOOR 1		FLOOR 3		FLOOR 0		FLOOR 2	
DATE	C_v [kW/K]	DATE	C_v [kW/K]	DATE	C_v [kW/K]	DATE	C_v [kW/K]
4-12-2014	0.11	2-12-2014	0.10	4-12-2014	0.10	3-12-2014	0.13
11-12-2014	0.10	4-12-2014	0.16	5-12-2014	0.15	4-12-2014	0.08
15-12-2014	0.13	9-12-2014	0.10	9-12-2014	0.10	9-12-2014	0.08
8-1-2015	0.14	15-12-2014	0.10	7-1-2015	0.10	15-12-2014	0.07
9-1-2015	0.12	18-12-2014	0.14	8-1-2015	0.11	7-1-2015	0.06
12-1-2015	0.11	5-1-2015	0.09	20-1-2015	0.10	8-1-2015	0.03
15-1-2015	0.13	7-1-2015	0.09	22-1-2015	0.17	20-1-2015	0.07
2-2-2015	0.11	8-1-2015	0.12	23-1-2015	0.08	22-1-2015	0.10
6-2-2015	0.16	9-1-2015	0.11	26-1-2015	0.08	26-1-2015	0.06
10-2-2015	0.09	12-1-2015	0.11	27-1-2015	0.13	27-1-2015	0.09
12-2-2015	0.10	13-1-2015	0.10	30-1-2015	0.08	2-2-2015	0.07
18-2-2015	0.10	15-1-2015	0.09	2-2-2015	0.08	3-2-2015	0.08
19-2-2015	0.11	19-1-2015	0.11	6-2-2015	0.11	10-2-2015	0.06
20-2-2015	0.11	22-1-2015	0.16	10-2-2015	0.11	17-2-2015	0.11
2-3-2015	0.08	23-1-2015	0.10	16-3-2015	0.13	18-2-2015	0.08
5-3-2015	0.11	26-1-2015	0.09	–	–	19-2-2015	0.10
-	-	27-1-2015	0.12	–	–	5-3-2015	0.05
-	-	2-2-2015	0.13	–	–	16-3-2015	0.06
-	-	6-2-2015	0.13	–	–	23-3-2015	0.10
-	-	10-2-2015	0.09	–	–	24-3-2015	0.14
-	-	11-2-2015	0.11	–	–	–	–
-	-	12-2-2015	0.09	-	–	–	–
-	-	17-2-2015	0.15	-	–	–	–
-	-	2-3-2015	0.10	-	–	–	–
-	-	3-3-2015	0.06	-	–	–	–
-	-	11-3-2015	0.10	-	–	–	–
-	-	16-3-2015	0.14	–	–	–	–
-	-	23-3-2015	0.19	–	–	–	–
AVERAGE	**0.11 ±0.010 (C_{v_aver})**	**AVERAGE**	**0.11 ±0.011 (C_{v_aver})**	**AVERAGE**	**0.11 ±0.015 (C_{v_aver})**	**AVERAGE**	**0.08 ±0.012 (C_{v_aver})**

average concentration in the floor at the beginning or end of the sampling period (grey lines) have been rejected. Again, none of those days fulfil the ASTM D6245-18 requirements and are not considered in Table 5 for the latter C_v estimations. In addition, those days where the initial value of the measured CO_2 concentration (C_I) of any of the sensors was less than [outdoors 400 ppm + 350 ppm] have also been discarded. Note that initial and final values of the concentrations of Table 3 show the difference between the indoor to outdoor concentrations.

Fig. 5 shows a couple of examples of the ACH_{decay} values calculated for two of those days of February 2015 fulfilling the ASTM D6245-18 requirements for the first floor. Logarithmic concentration values have been used to obtain a linear relationship between the logarithm of the tracer gas concentration [LN (measured CO_2 ppm - outdoors CO_2 ppm)] and the time in [h]. Next, the ACH_{decay} of each day was calculated via linear regression analysis, since the ACH_{decay} value corresponds to the slope of the estimated straight line. The rest of the ACH_{decay} results, regression equations and R^2 values of the February 2015 days that fulfil the requirements are shown in Table 4.

The average ACH_{decay_aver} for the first analysed winter (December 2014–March 2015) of each floor is the average of all the ACH_{decay} values of those days that meet all the requirements presented in the previous section 3.2 (see Table 5). The ACH_{decay} values of F1 and F3 of the second winter period analysed (December 2015–March 2016) can be seen in Table A.1 in Appendix A.

Only F1 and F3 have several winter days that completely fulfil the ASTM D6245-18 requirements. The uniformity requirement established by the Standard could not be fulfilled on any of the days in the analysed period on F0 and F2. However, as mentioned in the previous section, the uniformity requirement has been substituted by a proposed one (maximum limit of 10 °C for the daily average outdoor temperature) in order to accept some daily ACH_{decay} values for these floors. Furthermore, as shown in Fig. 2, each sensor on those floors has been assigned a portion of the total volume of each floor, while the infiltration heat loss coefficient (C_v) for each floor has been estimated using both Eq. (33) and Eq. (34). Note that in F0, the considered volume partitions do not complete the full volume. In this case, the C_v value obtained by Eq. (34) has been extrapolated to the complete volume of the floor (green contoured area).

Table 6 shows the ACH_{decay} values of each volume portion of both floors and the average ACH_{decay} values associated to each whole floor. The daily ACH_{decay_Vi} shown in Table 6 are calculated using the CO_2 ppm values measured by each independent sensor located in each of the considered sub-volumes of each floor. These ACH_{decay_Vi} values are then averaged per column (see last row of Table 6) and the $ACH_{decay\_aver\_Vi}$ values to be used in Eq. (34) are obtained. On the other hand, for F0 and F2 in Table 6, a column titled 'Daily ACH_{decay} Average' is also presented. These values are calculated daily, as for F1 and F3, using the averaged CO_2 concentration of the different sensors located in each floor. The last value of the column 'Daily ACH_{decay} Average' is the ACH_{decay_aver} to be used in Eq. (33), obtained by averaging all the values of this column, as done for F1 and F3.

The Daily ACH_{decay} average values of F0 and F2 of the second winter period (December 2015–March 2016) can be seen in Table A.2 in Appendix A.

Table 8
C_{v_aver} values for each floor by means of both Eq. (33) and Eq. (34) and the whole building C_{v_aver} value for the winter of 2014–2015.

Winter 2014–2015	FLOOR 0	FLOOR 1	FLOOR 2	FLOOR 3	BUILDING
C_{v_aver} [kW/K] (Eq. (33))	0.11 ± 0.015	0.11 ± 0.010	0.08 ± 0.012	0.11 ± 0.011	**0.41 ± 0.048**
C_{v_aver} [kW/K] (Eq. (34))	0.10 ± 0.013	–	0.08 ± 0.014	–	–

Finally, it must be commented that the daily ACH_{decay} values and average wind speed in the same period (18:00 h to 20:00 h) of those days fulfilling the ASTM D6245-18 requirements are correlated. The ACH_{decay} values depend on the indoor to outdoor temperature difference and on wind direction, but mainly on wind speed. In general, from Tables 5 and 6, it can be concluded that the higher the average wind speed, the higher the ACH_{decay} values.

4.2. Infiltration heat loss coefficient (C_v) calculation

Once the ACH_{decay} values for the days fulfilling the ASTM D6245-18 requirements have been estimated, it is possible to estimate the corresponding C_v values for each of those days, as shown in Table 7. Moreover, using the averaged ACH_{decay_aver} values in the last row of Tables 5 and 6, the infiltration heat loss coefficients of each floor can be estimated for the whole winter. Then, using Eq. (33) for F1 and F3 and both Eq. (33) and Eq. (34) for F0 and F2, it is possible to estimate the infiltration heat loss coefficient for each floor, as shown in the last row of Table 7.

As commented before, considering the building as a thermodynamic system, the HLC value is an extensive property of the system; thus, the sum of the individual HLC values of all floors is the HLC of the building. The same happening with the HLC happens also with the C_v. Then, the building infiltration heat loss coefficient could also be precisely estimated by summing all the C_v values of all the thermal zones of the building. As proven in section 3.1, when estimating the building C_v as the sum of the C_v values of the different thermal zones of the building, the effects of the mass exchanges due to infiltration through the walls/floors/ceilings between the different thermal zones are cancelled out in the summation process. Nevertheless, unless the analysed thermal zones are completely airtight between them in the whole building, the individual C_v values estimated for each thermal zone (floors in this case) have no physical meaning, since they are also considering the mass transmission between the floors. However, since for this analysed building, the thermal zones were different floors separated by continuous concrete slabs, the infiltration exchanges between floors can be considered to be very low, which means that the considered individual thermal zone C_v values are mainly due to the indoor to outdoor infiltration effects. Furthermore, the indoor temperature was homogeneous between floors (see results of [5]), making internal heat exchange effects low compared to the indoor to outdoor heat exchanges, thus also making the individual thermal zones HLC, C_v and UA value estimates meaningful.

Table 8 shows that similar C_{v_aver} values are obtained by means of both equations for F0 and F2. Although using Eq. (34) is a better approach for F0 and F2, using and programming Eq. (33) is easier in practice.

Since the difference is negligible for this case, only Eq. (33) values are considered for the second winter analysed in this work, as presented in Table 9.

Although the obtained C_{v_aver} results do not differ greatly between the two different winter periods, it can be seen that the confidence intervals are wider for the winter of 2015–2016. This is due to the higher variability between the daily estimated ACH_{decay} values in the second winter and due to a lower number of hourly estimates within the winter. These daily ACH_{decay} values could be affected by the wind speed effects. However, as commented in Appendix A, since there are no measured values for wind speed during this second winter period, it cannot be proved.

4.3. Decoupling the HLC into its transmission (UA) and infiltration (C_v) heat loss coefficients

In Table 10, decoupled UA and C_v (or C_{v_aver}) values are shown for each floor and for the whole building for the two analysed winters. Once the floor-by-floor HLC and C_v have been estimated, the decoupling of the HLC is carried out by applying Eq. (35). The measurement errors were propagated until the UA values have been obtained. In Table 10, the HLC, UA and C_v values are calculated and, in Table 11, the values per floor area have also been estimated.

4.4. Discussion

Several aspects of this method and the corresponding results in the tables can be discussed. For example, Tables 5 and 6 for the winter of 2014–2015, as well as the rest of Tables A.1 and A.2 (for the winter of 2015–2016) in Appendix A show a large variation in the daily ACH_{decay} values, depending on the day. In other words, the in-use HLC is not constant over time, since the C_v part can vary greatly from day to day. It is important to remark that these C_v values have been obtained based on the ACH_{decay} values estimated by means of the application of the ASTM D6245-18 guide, so they generally fulfil the reliability criteria stated in the guide. Then, converting the ACH_{decay} values to C_v values only requires them to be multiplied by the volume of the corresponding floor, the density of the air and the constant pressure specific heat of the air. Thus, the C_v values can be considered as reliable as the calculated ACH_{decay} values that fulfil the ASTM D6245-18 guide.

The ACH_{decay} estimations for F1 and F3 are reliable, since they

Table 9
C_{v_aver} values for each floor by means of Eq. (33) and the whole building C_{v_aver} value for the winter of 2015–2016.

Winter 2015–2016	FLOOR 0	FLOOR 1	FLOOR 2	FLOOR 3	BUILDING
C_{v_aver} [kW/K] (Eq. (33))	0.10 ± 0.027	0.10 ± 0.032	0.10 ± 0.025	1.14 ± 0.047	**0.44 ± 0.131**

Table 10
HLC, C_v and UA values for each floor and for the whole building for the two winters. The error was propagated until the UA values have been estimated. The percentage of the weight of the UA and C_v on the HLC are also presented.

		FLOOR 0	FLOOR 1	FLOOR 2	FLOOR 3	BUILDING
Winter 2014–2015	**HLC [kW/K]**	1.03 ± 0.102	1.60 ± 0.158	1.12 ± 0.100	1.34 ± 0.124	**5.09 ± 0.484**
	C_v [kW/K]	0.11 ± 0.015 (10.7%)	0.11 ± 0.010 (6.9%)	0.08 ± 0.012 (7.1%)	0.11 ± 0.011 (8.2%)	**0.41 ± 0.048 (8.1%)**
	UA [kW/K]	0.92 ± 0.087 (89.3%)	1.49 ± 0.148 (93.1%)	1.04 ± 0.088 (92.9%)	1.23 ± 0.113 (91.8%)	**4.68 ± 0.436 (91.9%)**
Winter 2015–2016	**HLC [kW/K]**	1.05 ± 0.164	1.66 ± 0.221	1.14 ± 0.148	1.42 ± 0.191	**5.27 ± 0.724**
	C_v [kW/K]	0.10 ± 0.027 (9.5%)	0.10 ± 0.032 (6.0%)	0.10 ± 0.025 (8.8%)	0.14 ± 0.047 (9.9%)	**0.44 ± 0.131 (8.3%)**
	UA [kW/K]	0.95 ± 0.137 (90.5%)	1.56 ± 0.189 (94%)	1.04 ± 0.123 (91.2%)	1.28 ± 0.144 (90.1%)	**4.83 ± 0.593 (91.5%)**

Table 11
HLC, C_v and UA values per unit floor area for each floor and for the whole building. For clarity, errors have not been included.

		Area [m^2]	HLC [W/K·m^2]	C_v [W/K·m^2]	UA [W/K·m^2]
Winter 2014–2015	FLOOR 0	391.65	2.63	0.28	2.35
	FLOOR 1	456.32	3.51	0.24	3.27
	FLOOR 2	604.61	1.85	0.13	1.72
	FLOOR 3	458.51	2.92	0.24	2.68
	BUILDING	**1911.09**	**2.66**	**0.21**	**2.45**
Winter 2015–2016	FLOOR 0	391.65	2.68	0.26	2.43
	FLOOR 1	456.32	3.64	0.22	3.42
	FLOOR 2	604.61	1.89	0.17	1.72
	FLOOR 3	458.51	3.10	0.31	2.79
	BUILDING	**1911.09**	**2.76**	**0.23**	**2.53**

completely fulfil the ASTM D6245-18 guide. However, since not all the building floors where structured equally, not all the requirements were fulfilled in two of them. For F0 and F2, the 10 % uniformity criteria has not been fulfilled and has been replaced by a no window opening criteria, according to an external low temperature criteria and visual checking of disturbances in the CO_2 concentration measurements. If we analyse the ACH_{decay} values for F0 in Table 6, it can be seen that V_1 and V_2 have very similar behaviour, while V_3 has nearly double the ACH_{decay} values compared to V_1 and V_2. If V_1 and V_2 (those volumes are close to each other) have similar ACH_{decay} values, it means that the CO_2 decay was not due to air exchanges between them. On the other hand, the V_3 of F0 has an old door that permits the children in the nursery to go out to the garden. This door is probably responsible for the much higher infiltration rates of V_3.

If the F2 ACH_{decay} rates are analysed in detail, two different behaviours can clearly be observed. V_1 and V_2 represent the north face offices and common north space that are connected by doors. If $ACH_{decay\_aver\_V1}$ and $ACH_{decay\_aver\_V2}$ are compared, they are very close, meaning that this subspace of F2 made up of V_1 plus V_2 has a similar ACH_{decay} behaviour. The same happens if $ACH_{decay\_aver\_V3}$ and $ACH_{decay\_aver\_V4}$ are analysed. In fact, there is a continuous brick wall separating both subspaces (north and south) and, logically, they have different behaviour. Since $V_1 + V_2 \sim V_3 + V_4$, if those two subspaces were treated separately, the C_v value calculated by Eq. (34) of Table 8 would be obtained. In this work, two options have been calculated for F0 and F2, as shown in Table 8, but since the difference is very small compared to the uncertainties we are working with, the easier to program Eq. (33) has been used for the decoupling calculations. Although the uncertainties associated to the estimations of the ACH_{decay} values of F0 and F2 might be bigger as they do not fulfil the 10 % uniformity criteria, after the above analysis and after checking the results, we consider them reliable enough to carry out the decoupling process of the HLC.

The two winters analysed have shown very interesting C_v results. In general, the third floor should be the one that shows the highest C_v results, since it is the floor most exposed to the wind. Moreover, it is logical that the floors that have distributions with big open spaces connecting internally north and south façades, such as F1 and F3, should have bigger C_v values, since it is easier for the air to enter, for example, from the north face and exit through the south face. This effect is usually lower for such floor distributions as F0 and F2, where there are many partition walls that hinder the indoor movement of the air. If the results are observed, it can be seen that the third floor is the one providing the highest C_v values. This effect can be more clearly seen in Table 11 when the C_v values are presented per floor area.

Furthermore, the results shown from Tables 7–9 lead to very interesting conclusions. If the individual daily C_v results are observed in Table 7, it is possible to find a considerable variation between the results obtained for the same floor. However, if the average C_v results are compared from Tables 8 and 9 for the two winter periods for the whole building, the results only differ by 7 %. So it can be concluded that, despite the variability of the obtained daily results, the final obtained values for the whole winters are stable and similar between the two winters.

Finally, regarding the HLC decoupling, if the results of Table 10 are observed, it can be seen that, floor by floor, the infiltration losses range is between 6.0 % and 10.7 % of the total heat losses for both winters. Thus, transmission losses range between 89.3 % and 94 %. This table provides highly valuable information about the effect of the retrofitting of the studied building. It is clear that, for this building, more than 90 % of heat losses are transmission losses, which suggests that the building should be better insulated to reduce the UA value. Moreover, Table 11 also shows very interesting results. From the results per unit area, it can be demonstrated that since the second floor is the one with the least wall area exposed to the exterior, the loss results obtained per floor square meter are the lowest. If the ground floor did not have a ventilated false ceiling, the first floor would have shown similar results to the second floor. However, due to the heat losses created by this ventilated false ceiling located between the ground floor and the first floor, the first floor shows the highest total losses, followed by the third floor, the floor most exposed to the wind effect.

5. Conclusions

This paper tests the internal validity of the decoupling of previously estimated floor-by-floor HLC values into their transmission heat loss coefficients (UA) and infiltration heat loss coefficients (C_v) by using the occupants' metabolic CO_2 concentration decay analysis to estimate the C_v, thus obtaining the value of the UA. The method proposed in this paper has been tested in an in-use office building, but it can also be considered valid for residential buildings. However, in that case, the CO_2 decay analysis should probably be done in the morning when the residential buildings have just been vacated by their occupants.

These authors consider the presented method is much more appropriate than the blower door test for this analysis, since the ACH_{decay} values are calculated in many different short testing periods over a long period and under real operating conditions. Unlike the blower door test, this method only needs the installation of simple sensors to be performed. Since the air quality sensors were already installed for the HLC analysis, it was only necessary to analyse the CO_2 concentration values provided from them. Moreover, since these sensors were distributed in different rooms of each floor, it has been possible to estimate the infiltration heat loss coefficients of the different thermal zones of the building. Last but not least, since the tracer gas is CO_2, it is not necessary to inject any gas into the building, which makes the method considerably more affordable in comparison to the blower door test or using other tracer gases.

The study was conducted using winter period data, when windows are usually closed (minimal air infiltrations) and the blinds are open (maximum solar gains). Thus, analysing the occupational CO_2 decay curves, the in-use infiltration Air Change per Hour (ACH_{decay}) rates have been estimated. These ACH_{decay} values have been used to calculate the C_v values for each floor and for the whole building, making it possible to

obtain the building envelope UA value using the following expression: UA = HLC - C_v.

Although the objective of the ASTM D6245-18 Standard is not to decouple the HLC into its UA and C_v parts, it provides a proven method to estimate the ACH_{decay} values of an occupied volume by means of metabolic CO_2 concentration measurements. As proven in this work, these ACH_{decay} values allow the C_v value of the studied volumes or thermal zones to be calculated. Depending on the distribution of the studied area, it is not easy to fulfil all the requirements established in the ASTM D6245-18 guide, in particular, those concerning the concentration uniformity throughout the whole studied area. However, analysing the floor-by-floor characteristics, acceptable ACH_{decay} results could be ensured, as proven in the calculation section.

Moreover, together with the average method, this method can provide the in-use HLC, UA and C_v values that could be used to obtain energy certificates for buildings in a more realistic approach. Then, the theoretical UA value of the building could be compared against the in-use UA value in order to know whether the construction has been carried out as designed. A similar comparison could be made between the in-use C_v value and the design C_v value. If the method is correctly integrated in the building's automation systems, it could be a cheap and non-disturbing method for the building users to understand the real behaviour of their building envelopes. In addition, once the in-use HLC (and both UA and C_v values) are available, decisions on where and how to optimally improve the building's energy performance can be made. This energy characterization of the building is a key point for the retrofitting process of existing buildings, since it allows the retrofitting needs to be evaluated, while still being aware of the impact of the retrofitting actions, and finally evaluating the savings and improvements obtained once the retrofitting has been accomplished. If the in-use HLC infiltration and/or the ventilation part (C_v) is too high, the window frames could be checked and improved if necessary, ventilation patterns could be optimized and window opening and closing patterns defined. If the UA must be reduced, optimized energy retrofitting strategies of the building envelope can be performed.

Finally, the extent of the information and data introduced in this work did not leave space for the decoupling analysis of the HLC values estimated after the rehabilitation. Therefore, the authors consider this paper could be interesting for future work where, apart from the infiltration heat loss coefficient, the ventilation heat loss coefficient must also be considered, since a ventilation system with heat recovery was installed in the building.

Authors Contributions

Irati Uriarte: Conceptualization, Methodology, Software, Validation, Investigation, Formal analysis, Data curation, Writing – original draft, Writing – review & editing. Aitor Erkoreka: Conceptualization, Methodology, Resources, Investigation, Writing – review & editing, Supervision, Project administration, Funding acquisition. Asier Legorburu: Conceptualization, Methodology, Software, Validation, Investigation, Formal analysis, Data curation, Writing – original draft. Koldo Martin-Escudero: Conceptualization, Writing – review & editing, Visualization. Catalina Giraldo-Soto: Conceptualization, Data curation, Writing – review & editing. Moises Odriozola-Maritorena: Conceptualization, Methodology, Writing – review & editing.

Declaration of competing interest

The authors declare that they have no known competing financial interests or personal relationships that could have appeared to influence the work reported in this paper.

Acknowledgements

This work was supported by the Spanish Ministry of Science, Innovation and Universities and the European Regional Development Fund (grant number RTI2018-096296-B-C22) through the MONITHERM project 'Investigation of monitoring techniques of occupied buildings for their thermal characterization and methodology to identify their key performance indicators', project reference: RTI2018-096296-B-C22 (MCIU/AEI/FEDER, UE). The corresponding author also acknowledges the support provided by the Education Department of the Basque Government through a scholarship granted to her to complete her PhD degree.

Appendix A

The procedure applied in section 4.1 and 4.2 for the winter period 2014–2015 has also been carried out for the second available winter period 2015–2016. Then, the ACH_{decay} results already shown in Table 5 for the winter period 2014–2015 are also presented for F1 and F3 for the winter 2015–2016 in Table A.1 of this section. This Table A.1 also includes the C_v results already shown for the winter 2014–2015 in Table 7, but for the winter 2015–2016.

Table A.1
The daily ACH_{decay}, C_v values and average wind speed (WS [m/s]) of all days fulfilling the ASTM D6245-18 requirements for F1 and F3. The last row presents the average ACH_{decay_aver} and C_{v_aver} values for F1 and F3 for the selected period (December 2015–March 2016). 95 % confidence intervals are presented for the averaged values using the t-student distribution.

FLOOR 1				FLOOR 3			
DATE	ACH_{decay}	WS [m/s]	C_v [kW/K]	DATE	ACH_{decay}	WS [m/s]	C_v [kW/K]
1-12-2015	0.10	–	0.06	4-12-2015	0.36	–	0.19
3-12-2015	0.33	–	0.19	14-12-2015	0.25	–	0.13
4-12-2015	0.05	–	0.03	8-1-2016	0.16	–	0.09
9-12-2015	0.09	–	0.05	12-1-2016	0.34	–	0.18
10-12-2015	0.09	–	0.05	13-1-2016	0.34	–	0.18
8-1-2016	0.12	–	0.07	23-2-2016	0.13	–	0.07
13-1-2016	0.36	–	0.20	25-2-2016	0.20	–	0.11
14-1-2016	0.22	–	0.12	–	–	–	–
22-2-2016	0.36	–	0.20	–	–	–	–
25-2-2016	0.22	–	0.13	–	–	–	–
1-3-2016	0.17	–	0.10	–	–	–	–
14-3-2016	0.14	–	0.08	–	–	–	–
15-3-2016	0.12	–	0.07	–	–	–	–

(continued on next page)

Table A.1 (*continued*)

FLOOR 1				FLOOR 3			
DATE	ACH_{decay}	WS [m/s]	C_v [kW/K]	DATE	ACH_{decay}	WS [m/s]	C_v [kW/K]
17-3-2016	0.11	–	0.06	–	–	–	–
18-3-2016	0.12	–	0.07	–	–	–	–
AVERAGE	**0.17 ± 0.056 (ACH_{decay_aver})**	**-**	**0.10 ± 0.032 (C_{v_aver})**	**AVERAGE**	**0.25 ± 0.086 (ACH_{decay_aver})**	**-**	**0.14 ± 0.047 (C_{v_aver})**

As done for F0 and F2 in Table 6 (section 4.1), the ACH_{decay} values are also estimated for the second winter. However, when studying the winter 2014–2015, it has already been proven that the difference between estimating the C_v values using Eq. (33) and Eq. (34) is insignificant. Then, for the second winter analysis, only the ACH_{decay_aver} has been estimated and Eq. (33) has been used to estimate the C_{v_aver} results, as done in F1 and F3. Thus, the same procedure used to estimate the ACH_{decay_aver} and the corresponding C_{v_aver} for winter 2014–2015, has also been applied in Table A.2 for the winter 2015–2016.

Table A.2
The daily ACH_{decay} average, C_v values and average wind speed (WS [m/s]) for F0 and F2. The last row presents the average ACH_{decay_aver} and C_{v_aver} values for F0 and F2 for the selected period (December 2015–March 2016). 95 % confidence intervals are presented for the averaged values using the t-student distribution.

DATE		FLOOR 0			FLOOR 2		
	T_{out}	Daily ACH_{decay} average	WS [m/s]	C_v [kW/K]	Daily ACH_{decay} average	WS [m/s]	C_v [kW/K]
1-12-2015	7.37	–	–	–	0.14	–	0.09
2-12-2015	9.00	0.15	–	0.06	–	–	–
11-1-2016	10.92	–	–	–	0.18	–	0.11
12-1-2016	7.98	–	–	–	0.12	–	0.08
13-1-2016	8.35	–	–	–	0.16	–	0.10
14-1-2016	10.58	0.18	–	0.07	–	–	–
25-2-2016	9.48	0.33	–	0.13	0.14	–	0.09
7-3-2016	6.20	–	–	–	0.18	–	0.12
8-3-2016	6.99	0.34	–	0.13	0.27	–	0.17
11-3-2016	8.67	0.20	–	0.08	–	–	–
14-3-2016	8.22	0.23	–	0.09	0.10	–	0.07
15-3-2016	10.13	0.27	–	0.11	0.10	–	0.07
Average		**0.24 ± 0.069 (ACH_{decay_aver})**	**-**	**0.10 ± 0.027 (C_{v_aver})**	**0.16 ± 0.040 (ACH_{decay_aver})**	**-**	**0.10 ± 0.025 (C_{v_aver})**

There were no wind speed measured data for this second winter. So it has been impossible to find a correlation between the ACH_{decay} and the wind speed for this second winter period. However, since the winter 2014–2015 had good measured wind speed data, some conclusions could be made here.

References

[1] European Parliament, Directive 2018/844/EU of the European Parliament and of the council of 19 June 2018 on the energy performance of buildings (recast), Official Journal of the European Communities 61 (2018) 75–91.
[2] D. Calì, T. Osterhage, R. Streblow, D. Müller, Energy performance gap in refurbished German dwellings: lesson learned from a field test, Energy Build. 127 (2016) 1146–1158, https://doi.org/10.1016/j.enbuild.2016.05.020.
[3] P.X.W. Zou, D. Wagle, M. Alam, Strategies for minimizing building energy performance gaps between the design intend and the reality, Energy Build. 191 (2019) 31–41, https://doi.org/10.1016/j.enbuild.2019.03.013.
[4] D. Johnston, D. Miles-Shenton, D. Farmer, Quantifying the domestic building fabric 'performance gap', Build. Serv. Eng. Technol. 36 (2015) 614–627.
[5] I. Uriarte, A. Erkoreka, C. Giraldo-Soto, K. Martin, A. Uriarte, P. Eguia, Mathematical development of an average method for estimating the reduction of the Heat Loss Coefficient of an energetically retrofitted occupied office building, Energy Build. 192 (2019) 101–122, https://doi.org/10.1016/j.enbuild.2019.03.006.
[6] K. Chávez, D.P. Ruiz, M.J. Jiménez, Dynamic integrated method applied to assessing the in-situ thermal performance of walls and whole buildings. Robustness analysis supported by a benchmark set-up, Appl. Therm. Eng. 152 (2019) 287–307.
[7] O. Mejri, E.P. Del Barrio, N. Ghrab-Morcos, Energy performance assessment of occupied buildings using model identification techniques, Energy Build. 43 (2011) 285–299.
[8] Y. Li, Y. Rezgui, A novel concept to measure envelope thermal transmittance and air infiltration using a combined simulation and experimental approach, Energy Build. 140 (2017) 380–387.
[9] M.H. Sherman, W.R. Chan, Building Air Tightness: Research and Practice, Building Ventilation: the State of the Art, 2006, pp. 137–162.
[10] A.K. Persily, Field measurement of ventilation rates, Indoor Air 26 (2016) 97–111.
[11] J.F. Belmonte, R. Barbosa, M.G. Almeida, CO2 concentrations in a multifamily building in Porto, Portugal: occupants' exposure and differential performance of mechanical ventilation control strategies, J. Build. Eng. 23 (2019) 114–126.
[12] W. Lin, L. Li, X. Liu, T. Zhang, On-site measurement and numerical investigation of the airflow characteristics in an aquatics center, J. Build. Eng (2020) 101968.
[13] Y. Liu, P.K. Misztal, J. Xiong, Y. Tian, C. Arata, W.W. Nazaroff, A.H. Goldstein, Detailed investigation of ventilation rates and airflow patterns in a northern California residence, Indoor Air 28 (2018) 572–584.
[14] A. Meiss, J. Feijó-Muñoz, The energy impact of infiltration: a study on buildings located in north central Spain, Energy Effic 8 (2015) 51–64.
[15] R. Claude-Alain, F. Foradini, Simple and cheap air change rate measurement using CO2 concentration decays, Int. J. Vent. 1 (2002) 39–44.
[16] A. Sfakianaki, K. Pavlou, M. Santamouris, I. Livada, M. Assimakopoulos, P. Mantas, A. Christakopoulos, Air tightness measurements of residential houses in Athens, Greece, Build. Environ. 43 (2008) 398–405.
[17] A. Hayati, M. Mattsson, M. Sandberg, Single-sided ventilation through external doors: measurements and model evaluation in five historical churches, Energy Build. 141 (2017) 114–124.
[18] G. Hong, B.S. Kim, Field measurements of infiltration rate in high rise residential buildings using the constant concentration method, Build. Environ. 97 (2016) 48–54.
[19] A. Kabirikopaei, J. Lau, Uncertainty analysis of various CO2-Based tracer-gas methods for estimating seasonal ventilation rates in classrooms with different mechanical systems, Build. Environ. (2020) 107003.
[20] C.Y. Chao, M.P. Wan, A.K. Law, Ventilation performance measurement using constant concentration dosing strategy, Build. Environ. 39 (2004) 1277–1288.
[21] J.T. Reardon, M.R. Atif, S. Chia-yu, Tracer gas measurements for ventilation, air movement and air infiltration in a four-sided atrium office building, Int. J. Vent. 1 (2002) 13–22.
[22] C.J. Ghazi, J.S. Marshall, A CO2 tracer-gas method for local air leakage detection and characterization, Flow Meas. Instrum. 38 (2014) 72–81.
[23] E. Zender, –Świercz, Improvement of indoor air quality by way of using decentralised ventilation, J. Build. Eng. 32 (2020) 101663.
[24] S. Cui, M. Cohen, P. Stabat, D. Marchio, CO2 tracer gas concentration decay method for measuring air change rate, Build. Environ. 84 (2015) 162–169.
[25] S. Guillén-Lambea, B. Rodríguez-Soria, J.M. Marín, Air infiltrations and energy demand for residential low energy buildings in warm climates, Renew. Sustain. Energy Rev. 116 (2019) 109469.

[26] Khemet B., Richman R., An empirical approach to improving preconstruction airtightness estimates in light framed, detached homes in Canada, J. Build. Eng. 33 101433.
[27] K. Ghoreishi, A. Fernández-Gutiérrez, F. Fernández-Hernández, L. Parras, Retrofit planning and execution of a Mediterranean villa using on-site measurements and simulations, J. Build. Eng (2020) 102083.
[28] M. Senave, G. Reynders, P. Bacher, S. Roels, S. Verbeke, D. Saelens, Towards the characterization of the heat loss coefficient via on-board monitoring: physical interpretation of ARX model coefficients, Energy Build. 195 (2019) 180–194.
[29] S. Roels, P. Bacher, G. Bauwens, S. Castaño, M.J. Jiménez, H. Madsen, On site characterisation of the overall heat loss coefficient: comparison of different assessment methods by a blind validation exercise on a round robin test box, Energy Build. 153 (2017) 179–189, https://doi.org/10.1016/j.enbuild.2017.08.006.
[30] A. Erkoreka, E. Garcia, K. Martin, J. Teres-Zubiaga, L. Del Portillo, In-use office building energy characterization through basic monitoring and modelling, Energy Build. 119 (2016) 256–266, https://doi.org/10.1016/j.enbuild.2016.03.030.
[31] H.P. Díaz-Hernández, P.R. Torres-Hernández, K.M. Aguilar-Castro, E.V. Macias-Melo, M.J. Jiménez, Data-based RC dynamic modelling incorporating physical criteria to obtain the HLC of in-use buildings: application to a case study, Energies 13 (2020) 313.
[32] F. Alzetto, D. Farmer, R. Fitton, T. Hughes, W. Swan, Comparison of whole house heat loss test methods under controlled conditions in six distinct retrofit scenarios, Energy Build. 168 (2018) 35–41.
[33] ASTM D6245-18, Standard Guide for Using Indoor Carbon Dioxide Concentrations to Evaluate Indoor Air Quality and Ventilation, 2018. West Conshohocken, PA.
[34] ASTM E741-11, Standard Test Method for Determining Air Change in a Single Zone by Means of a Tracer Gas Dilution, 2017.
[35] Y. Cengel, Heat and Mass Transfer: Fundamentals and Applications, McGraw-Hill Higher Education, 2014.
[36] S. Van Buggenhout, T.Z. Desta, A. Van Brecht, E. Vranken, S. Quanten, W. Van Malcot, D. Berckmans, Data-based mechanistic modelling approach to determine the age of air in a ventilated space, Build. Environ. 41 (2006) 557–567.